Progress Report on
E110 Post-Quench Ductility Test Program

Y. Yan, T. Burtseva and M.C. Billone
Argonne National Laboratory
May 31, 2003

Summary

A series of pre-test characterizations, oxidation tests and post-test characterizations are in progress to determine the root cause of the low transition ECR values for breakaway oxidation and high-hydrogen uptake of E110 in steam, particularly at 1000°C. Based on previously published work, E110 experiences breakaway oxidation at ECR < 6% and high-hydrogen uptake for ECR > ≈6% at 1000°C during two-sided oxidation tests. The transition ECR values for E110 are higher for higher test temperatures. The transition ECR for hydrogen uptake and embrittlement is higher for one-sided vs. two-sided steam oxidation test conditions. Both breakaway oxidation and high hydrogen uptake appear to be due to the transition from tetragonal oxide (lustrous black) to local and global regions of the more brittle monoclinic oxide (grayish-white). In contrast, the Zr-1Nb alloy M5 exhibits good performance in steam at 1000-1200°C for test times corresponding to >17% ECR: the oxide layer formed on M5 is uniform and lustrous black; and the hydrogen uptake is low (<50 wppm). Easily observable and measurable differences between as-received E110 vs. M5 tubing are the larger surface roughness (≈0.4 μm vs. ≈0.1 μm), smaller diameter, thicker wall (0.7 mm vs. 0.6 mm), and lower oxygen content (≈500 wppm vs. ≈1400 wppm) for E110. Otherwise, the two materials appear very similar with regard to concentration of alloying elements and impurities to the extent that such impurities can and have been measured and reported. Yet, based on the dramatic difference in oxidation behavior, there must be a fundamental difference or combination of factors that contributes to the poor performance of E110, especially at 1000°C.

The ANL test results at 1000°C indicate the following evolution for as-received E110 cladding: very early initiation of small (<100 μm), isolated white spots (presumed to be monoclinic oxide) in a predominately black oxide (presumed to be tetragonal oxide); growth of these white spots into visible white-silver nodes; growth, interconnection and cracking of these nodes, accompanied by significant hydrogen uptake; and increased surface-area coverage of the "white" oxide followed by delamination, spallation and very high hydrogen uptake. The limited metallography performed indicates that most, if not all, of the oxide delaminates down to the bare metal, followed by re-oxidation. The initiating process is similar at 1100°C, except that the white oxide nodes tend to remain isolated and/or grouped into regions up to much higher ECR values (>15%). Such behavior is distinctly different from breakaway oxidation observed on the surface of other alloys: macroscopic regions of monoclinic oxide initiating on the outer surface of the oxide, followed by partial delamination and spallation, after long periods of time (1-3 hours) at 1000°C.

In an effort to better understand the behavior of E110, several processes were used to modify the surface, the surface substrate, and up to ≈100 μm into the metal to assess their contributions to the low transition ECR values of E110. In parallel to these studies, preliminary

SEM and TEM have been performed on as-received E110 for comparison to published results for M5. The effects of three E110 sample preparations were investigated: polishing to smooth out the surface roughness and eliminate possible surface impurities; etching to remove surface oxides and impurities (≈14 μm) while leaving a rougher-than-polished surface; and machining followed by polishing to remove the surface and substrate (25-110 μm) from the outer and/or inner surface. Of these three techniques, machining-and-polishing gave marginally better results than polishing alone, which proved to be far superior to etching and far superior to as-received cladding performance, based on tests at 1000°C and ≥5% ECR. The oxidation performance of pre-etched E110 appears to be highly sensitive to the HF concentration in the etchant and the etching time, more so than the other alloys tested under the same conditions. Most of the tests with pre-etched E110 resulted in higher surface-area coverage of monoclinic oxide than experienced by as-received E110 samples. Performance indicators included size (≤100 μm) of white spots viewed at high magnification, visual appearance of the outer-surface oxide (e.g., area fraction of monoclinic oxide formation, delamination and spallation), metallography to determine the depth of the delamination, and hydrogen uptake.

In order to better compare the behavior of E110 and M5 in the ANL oxidation test apparatus, ≈115 μm was machined from the as-received inner surface of E110 and both inner and outer surfaces were polished. This process results in comparable thickness (≈0.6 mm) and outer-surface finish for both E110 and M5. Based on results from 1000°C and 1100°C oxidation tests, the weight gain kinetics of E110 compare favorably to the M5 kinetics during the time interval in which the E110 oxide layer remains black and uniform. Both materials have a weight-gain coefficient at 1000°C that is 30-40% less than predicted by the Cathcart-Pawel model. At 1100°C, the weight-gain coefficients for E110 and M5 are closer to the Cathcart-Pawel model prediction.

While polishing and machining-and-polishing extend the time for E110 breakaway oxidation from ≈300-s (5% ECR) to ≈1000-s (9% ECR) hold times at 1000°C, this time falls far short of the hold times (≈2400 s) at 1000°C for which the M5 oxide remains uniform and black. The M5 tests were not run long enough to determine breakaway oxidation for this alloy during two-sided oxidation at 1000°C. Based on a one-sided M5 test at 1000°C, extensive monoclinic oxide formation is observed on the outer surface of the oxide layer after ≈3 hours in steam.

The tests performed to date at ANL confirm previously published E110 oxidation behavior at 1000°C, demonstrate that surface polishing improves the behavior of E110, show that pre-etching can degrade the oxidation performance of E110, but strongly suggest that the oxide instabilities on E110 arise from more than just surface roughness and surface/substrate chemistry. Ring compression tests will be performed to confirm embrittlement vs. ECR and hydrogen content. SEM and TEM analyses of as-received E110 tubing are in progress both at ANL and at RRC-KI/RIAR to determine differences in E110 microstructure that may explain the dramatic differences in behavior between E110 and M5. The focus of the TEM investigation is the characterization of Nb precipitate size and distribution, as well as the characterization of second-phase precipitate size, distribution and chemical composition.

1. Introduction

A series of tests have been conducted to determine the root cause or causes of early breakaway oxidation on E110 and embrittling hydrogen uptake during high temperature steam oxidation. Two-sided steam oxidation tests have been conducted on as-received E110 and modified E110 tubing samples. Many of these tests were run at 1000°C for hold times < 420 s. The Cathcart-Pawel calculated ECR for these conditions (including the 75-s temperature ramp) is ≤6%, relative to the as-received E110 thickness (0.71 mm). Based on results of other investigators, the transition ECR between ductile and brittle behavior is in the range of 5-7% ECR following two-sided steam oxidation at 1000°C. Also based on these studies, transition ECR values are higher for higher oxidation temperatures, for faster temperature ramp rates and for one-sided vs. two-sided tests at 1000-1200°C. The transition between ductile and brittle behavior appears to correlate with the abrupt increase in hydrogen uptake from ≈100-1000 wppm.

Initially, several one-sided steam-oxidation tests were conducted at 1100°C with as-received E110 samples. Based on the results of these tests, the sequence of events leading to embrittlement of E110 appears to be: very early formation of small (<100 μm) white spots of monoclinic oxide within a black tetragonal oxide matrix, growth of these white spots into nodules, partial cracking and interconnection of the nodules into regions of monoclinic oxide, crack extension through the thickness of the monoclinic nodules to the base metal and significant hydrogen uptake concurrent with steam/base-metal reaction. As this behavior is localized, rather than uniform, sample weight gain and "measured" ECR do not appear to be meaningful parameters for data correlation. Time at temperature – including the temperature ramp – appears to be more meaningful. Based on several two-sided tests at 1000°C up to 10% ECR, extensive monoclinic oxide formation, delamination, spallation, and high-hydrogen uptake (>4000 wppm) were observed as the hold time was increased to ≈1400 s. These tests confirm previous observations that E110 is more challenged in steam at 1000°C than at >1050°C.

In order to better understand the characteristics of E110 that may cause it to behave so differently from other zirconium-based cladding alloys (Zry-2, Zry-4, ZIRLO, and M5), tests were designed to isolate material factors (surface roughness, surface chemistry, substrate chemistry and microstructure, bulk chemistry and microstructure) that may be responsible for early-in-time breakaway oxidation of E110. In assessing the possible roles of E110 surface, substrate and bulk, it should be emphasized that the depth of metal consumed as oxide is relatively small for the ECR range of interest. At 5, 10 and 15% ECR, the predicted metal thickness consumed on the inner and outer surfaces is ≈15 μm, ≈30 μm and ≈45 μm, respectively. The wall thickness of the as-received tubing is 710 μm. In terms of direct interaction with steam, the surface and substrate (near-surface) regions are most important. The bulk material below the substrate does experience oxygen uptake and may influence the oxide/metal surface and oxide layer through diffusion of elements (e.g., Nb) from the bulk to the oxidizing surface to the oxide.

2. E110 Chemistry and Sample Preparation

Ten E110 cladding tube segments were supplied by Fortum. Two of these were etched-and-anodized. Although two oxidation tests were performed with anodized samples, the results indicated steam oxidation behavior essentially the same as for non-anodized tubing. The results described in this report are from tests conducted with non-anodized tubing, which has a cladding outer diameter of 9.17 mm and a wall thickness of 0.71 mm.

2.1 E110 Bulk Chemistry

Table 1 lists the measured concentrations of alloying elements and impurities in E110, as well as the E110 specifications reported by P. V. Shebaldov et al. [2]. Although the Fe and C contents are higher than the "typical" values, the chemistry of the Fortum-supplied E110 is essentially within E110 specifications. For comparison, M5 specifications [1] are also listed.

Table 1 Chemical Composition of E110 used in ANL Oxidation Studies vs. M5

Element	M5 Range [1]	E110 Specification [2] (Typical Values)	Fortum E110 Measured by CONAM	Fortum E110 Measured by ANL
Zr, wt.%	balance	balance	balance	balance
Nb, wt.%	0.8-1.2	0.9-1.1	1.03±0.01	---
O, wt.%	0.11-0.17	<0.10 (0.05-0.07)	0.05	0.0505
Fe, wppm	150-600	<500 (140)	400-700	---
Cr, wppm	---	<200 (<30)	<100	---
Sn, wppm	---	<500 (<100)	200	---
S, wppm	10-35	---	10-40	---
C, wppm	<100	<200 (<40-70)	110-160	---
Hf, wppm	---	<500 (300-400)	100	---
Si, wppm	---	<200 (46-90)	100	---
Ni, wppm	---	<200 (30-39)	<100	---
Pb, wppm	---	<50	<100	---
W, wppm	---	---	100	---
Ta, wppm	---	---	<100	---
N, wppm	---	<60 (<30-40)	50-60	-
H, wppm	---	<15 (4-7)	4.1-5.9	2.1

1. J.-P. Mardon et al., "Influence of Composition and Fabrication Process on Out-of-Pile and In-Pile Properties of M5 Alloy," Zirconium in the Nuclear Industry: 12th International Symposium, ASTM STP 1354 (2000) pp 505-524.

2. P. V. Shebaldov et al., "E110 Alloy Cladding Tube Properties and Their Interrelationship with Alloy Structure-Phase Condition and Impurity Content," Zirconium in the Nuclear Industry: 12th International Symposium, ASTM STP 1354 (2000) pp 545-559.

2.2 As-received, Polished and Etched E110 Outer Surfaces

Figure 1a shows a 50x image of the as-received E110 outer surface. At lower magnification, both axial and circumferential striations or grooves – deeper than the random roughness – are evident. At the 50x magnification, the circumferential grooves, as well as the roughness between the grooves, are apparent. For as-received and machined samples, surface polishing (see Fig. 1b) was performed with 9-μm-grain Al_2O_3 paper for 2 minutes, followed by 3-μm-grain paper for 3 minutes. Figure 1c shows the effects of etching: decrease in random roughness; and axial and circumferential grooves still evident. The old etching solution was initially 40 ml HF + 40 ml HNO_3 + 100 ml lactic acid + 100 ml distilled water. About 14 μm of the inner and outer surfaces were removed during the etching. The etched outer surface has a roughness between the as-received (0.35 μm) and the polished (0.13 μm) samples.

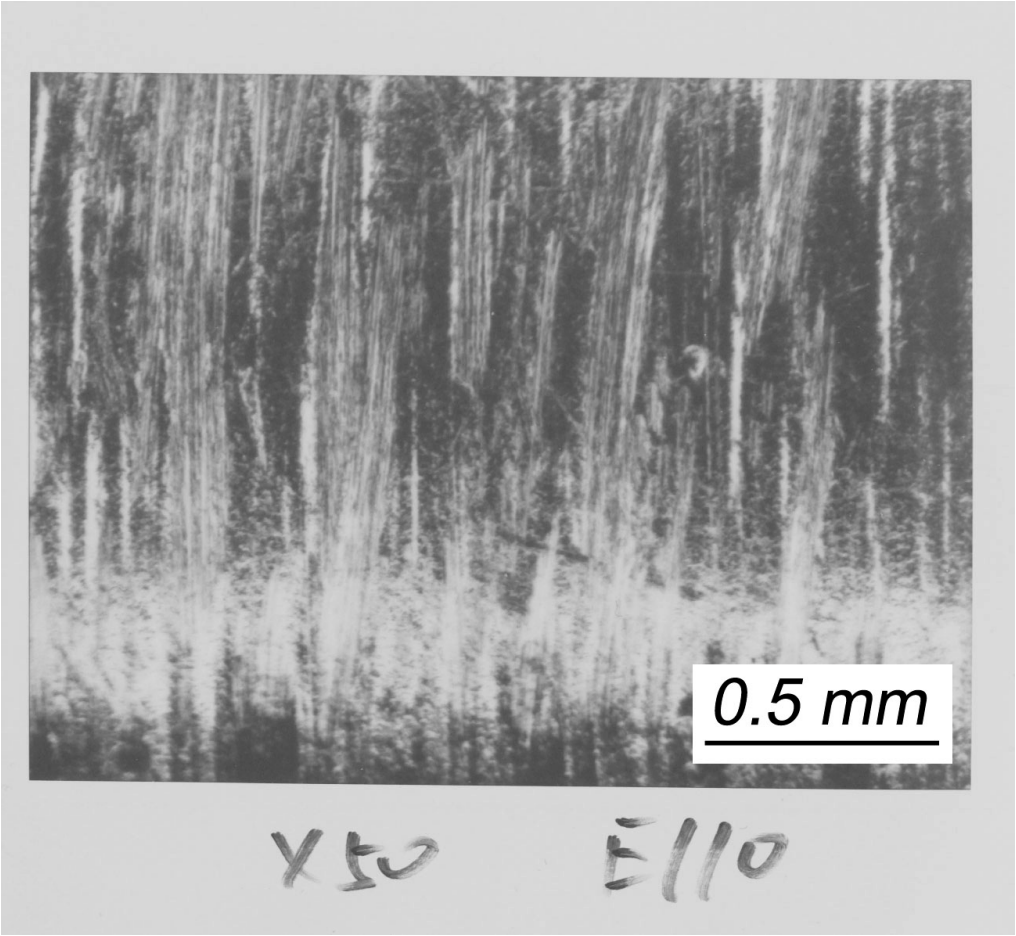

Fig. 1a. High-magnification (50x) image of the outer surface of as-received E110. Vertical direction in photograph corresponds to the circumferential tube direction. Measured surface roughness is 0.35 μm.

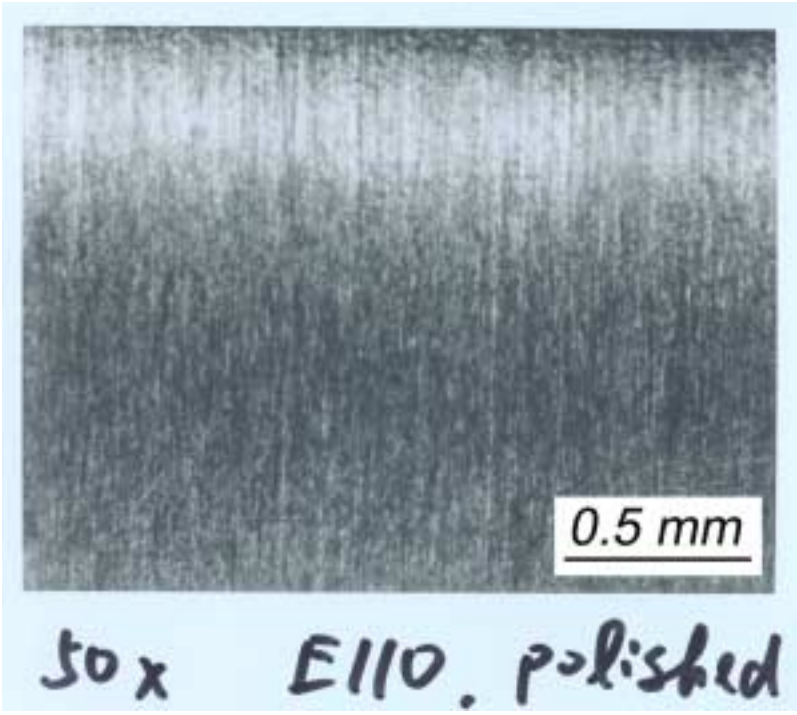

Fig. 1b. High-magnification (50x) image of the outer surface of polished E110. Measured surface roughness is 0.13 μm.

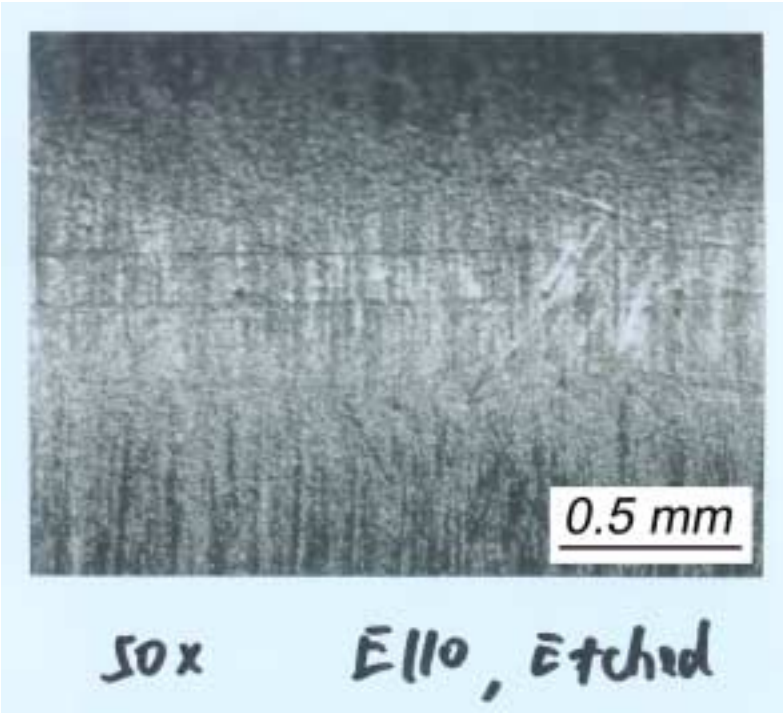

Fig. 1c. High magnification (50x) image of the outer surface of etched E110 surface. The etching solution consisted of HF + HNO_3 + lactic acid + distilled water.

2.3 Preliminary SEM/TEM Characterization of As-received E110

The results of the preliminary SEM/TEM characterization of as-received E110 will be documented in a separate report. However, to put this work in the proper perspective, the TEM specimen is a thin foil about half the wall thickness of the tubing and ≈3 mm in diameter. Areas focused on are less than 0.5×0.5 μm and the interpretation of results is highly dependent on the details of the techniques used. More samples and more detailed investigations would be required to generalize about the "average" microstructure of a long E110 cladding tube. The summary of the preliminary characterization is as follows:

The average grain size was determined to be 4.7 μm, which is consistent with the 3-5 μm reported for M5 in Ref. 1.

Nb-Fe-rich precipitates >100 nm were observed, which is consistent with the 100-200 nm Zr(Nb, Fe, Cr) precipitates reported for M5 in Ref. 1.

Nb-rich precipitates ≈40 nm were observed, which is consistent with the 50-nm beta-phase Zr-Nb precipitates reported for M5 in Ref. 1.

Defects (e.g. strain fields around particles) were observed, which was not reported for M5 in Ref. 1.

A non-uniform cluster of precipitates was observed at one location, while the precipitates documented for M5 in Ref. 1 were uniformly distributed. If clusters of Nb-rich precipitates do characterize the bulk of the material, such precipitates could negatively impact the steam-oxidation behavior of E110. However, more regions of E110 would have to be examined to determine if such clusters are rare or characteristic of the material. Also, M5 TEM planned by ANL would have to be completed so that the two materials could be compared using the same techniques.

3. Test Results for As-Received E110

3.1 Results of Two-sided Steam Oxidation Tests Conducted at 1000°C

Table 2 summarizes the two-sided, steam-oxidation tests conducted at ANL on as-received E110 cladding samples to determine the effects of time at 1000°C on the uniformity of the oxide layer and the hydrogen pickup. The test samples are nominally 25-mm long. The Cathcart-Pawel (CP) correlation was used to calculate the normalized weight gain due to oxygen pickup and the corresponding ECR. Because of the relatively early-in-time nodular breakaway oxidation and the resulting nonuniformity of the oxide layer, no attempts were made to determine the "experimental" ECR based on the Zr consumed. Although the sample weights before and after the test were recorded, the more brittle white regions tend to partially flake off during the test and during post-test handling, thus rendering sample weight change as an unreliable method of determining ECR experimentally. Caution should be used in comparing the CP-calculated ECR values listed with those determined experimentally or by other correlations.

As there are really 3 weight-gain coefficients that could be deduced from the CP data, it is necessary to specify which weight gain coefficient was used. Let Δw_o = normalized weight gain in mg/cm^2, t = time in seconds, and k = the weight gain coefficient for isothermal oxidation. For parabolic kinetics associated with the protective black tetragonal oxide formation, the relevant equation is:

$$\Delta w_o = k\, t^{0.5} \tag{1}$$

and the corresponding ECR (%) for the E110 geometry and two-side oxidation is

$$\mathrm{ECR} = 1.235\, \Delta w_o \tag{2}$$

The Cathcart-Pawel correlations for 1000°C oxidation give k = 0.2242 assuming the oxide layer is stoichiometric, k = 0.2190 accounting for the hypostoichiometric nature of the oxide layer, and k = 0.2093 as a best fit to the CP data at 1000°C. Consistent with the correlations in the summary of CP report (ORNL/NUREG-17, Aug. 1977) and with what most researchers report as the Cathcart-Pawel correlation, k = 0.2242 is used to determine the predicted weight gain and ECR at 1000°C. Note that the CP values for Δw_o and ECR listed in the tables are determined by integrating the rate form of this equation over the temperature history determined from thermal benchmark tests with thermocouples (TCs) welded directly onto the sample. All of the calculated results in Table 2, with the exception of Test EU#8, are based on integration of the average of the temperature histories for the two benchmark TCs, whose readings are shown in Fig. 2. The ramp time from 300°C to 1000°C is about 75 s, with most of that time spent at 900 to 1000°C. For EU#8, fast ramp-rate parameters were used, such that the ramp rate (≈100°C/s) was essentially instantaneous.

Table 2 Two-Sided Steam Oxidation Tests Conducted at 1000°C with As-Received E110 Cladding Samples; outer diameter is 9.17 mm; wall thickness is 0.71 mm; t_s = hold time at 1000°C; ramp from 300°C to 1000°C is shown in Fig. 2; Δw_p = CP-model-predicted normalized weight gain; ECR = 1.235 Δw_p; hydrogen samples were cut from center (C) and off-center (OC) sample locations; sample length is ≈25 μm

Test ID#	t_s s	Pred. ECR %	Pred. Δw_p mg/cm^2	H Content wppm	Sample Condition Observations
EU#10	5	1.8	1.49	---	Uniform black oxide layer White spots ≤50 μm (Fig. 3)
EU#9	290	5.0	4.07	---	Extensive monoclinic oxide around welded TCs (Fig. 4)
EU#12	290	5.0	4.07	120±45 (C)	Nonuniform oxide (Fig. 5) Delamination (Fig. 6)
EU#11	290 at 950°C	<5	<4	---	Oxide surface (Fig. 7) may be worse than EU#12 sample
EU#36	395	5.8	4.67	7±3 (C) 44±7 (OC)	Nonuniform oxide layer
EU#38	625	7.1	5.78	80±40 (C) 90±90 (C) 420±160 (OC)	Axial distribution of hydrogen content (Fig.8)
EU#40	825	8.1	6.59	540±80 (C) 1430±110 (OC)	Delamination-spallation from half the sample
EU#8	1400	10.4	8.39	4230±250 (C)	Extensive delamination-spallation (see Fig. 9)

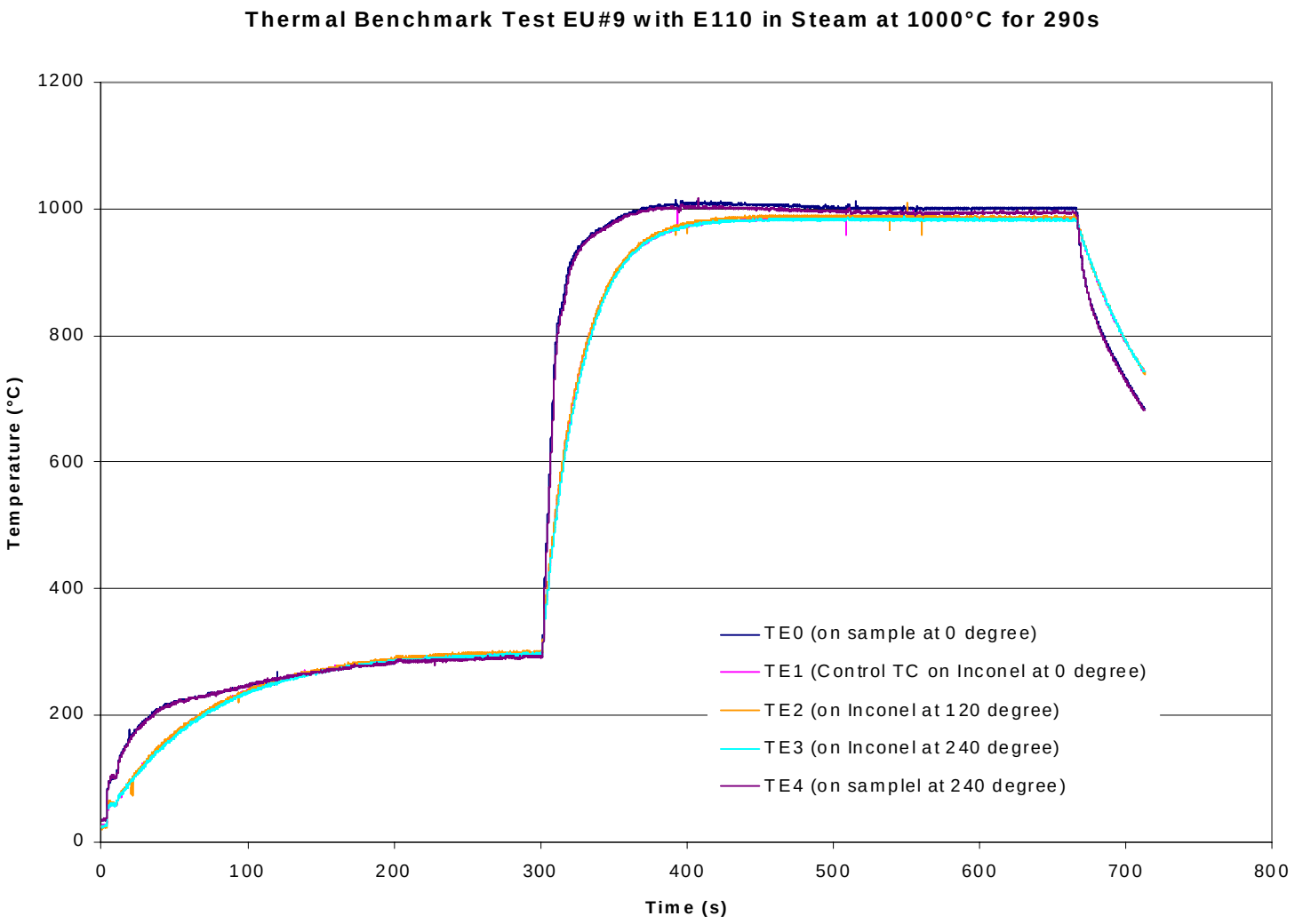

Fig. 2. Results of thermal benchmark test EU#9 with E110 sample in steam (two-sided oxidation) for a hold temperature of 1000°C.

3.1.1 Early-time Results (EU#10)

After the 75-s ramp and the 5-s hold time, the oxide layer on the EU#10 sample appears to be lustrous-black and uniform. However, high-magnification images (Fig. 3) reveal the presence of "white spots" in a black matrix. It is assumed that these are initiation sites for nodular oxidation, for which the oxide behavior is consistent with the behavior of monoclinic oxide.

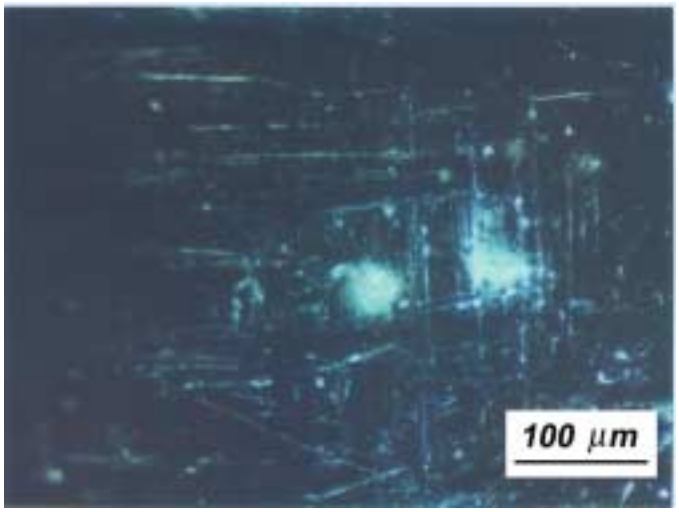

Fig. 3. Initiation of sites for nodular monoclinic oxide growth on as-received E110 after the 75-s ramp to 1000°C and the 5-s hold time at 1000°C.

3.1.2 Results after 290-s Hold-time at 1000°C (EU#9 and 12) and 950°C (EU#11)

Thermal-benchmark Test EU#9 had 2 TCs welded directly onto the outer surface of the sample. Unlike the other alloys tested, significant buildup of monoclinic oxide occurred around the welded TCs (Fig. 4). Because of the negative effects of the welded TCs on the outer surface oxide of E110 and the practicalities of cost and time of welding TCs to each sample, this approach was abandoned. Test EU#12 was run under the same time-temperature conditions as EU#9, but without TCs welded onto the sample. It developed local regions of nodular oxidation as well as interconnecting regions (Fig. 5). Because surface images may be deceiving with respect to the depth of the monoclinic oxide, metallography was performed on another sample tested under the same conditions. Figure 6 shows that there are regions on the sample with local delamination of the oxide essentially down to the base metal. This result is consistent with the measured hydrogen concentration of 120±45 wppm for the EU#12 sample.

An additional test (EU#11) was run at 950°C for the same 290-s hold time. Based on calculational models, both the weight gain and ECR should have been smaller for this sample than for the sample tested at 1000°C. However, the extent of monoclinic oxide formation and cracking appears greater than for the sample tested at 1000°C.

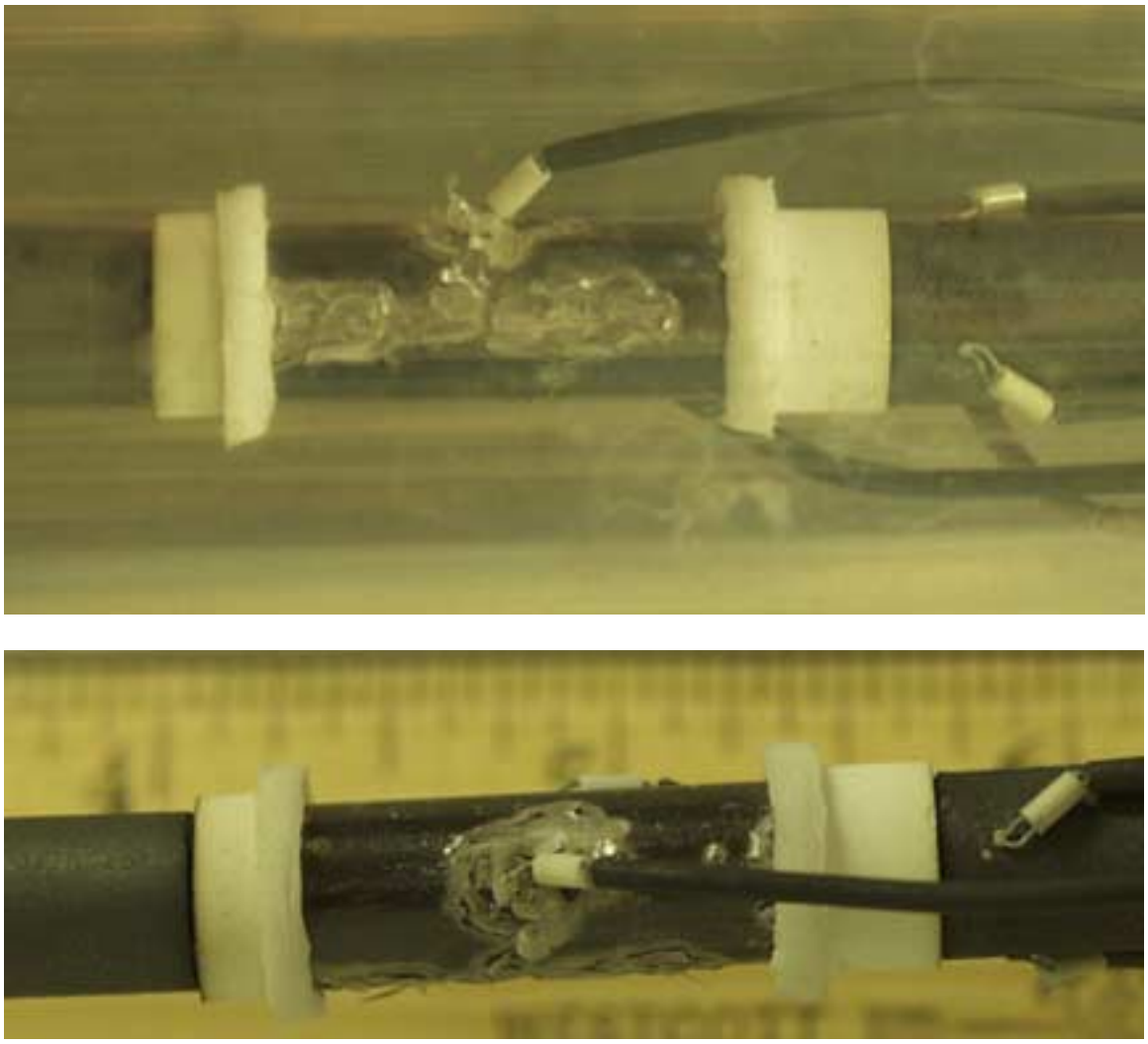

Fig. 4. Extensive monoclinic oxide formation and breakaway oxidation observed after thermal benchmark test EU#9 (1000°C for 290 s), especially in the region around the Type S thermocouples welded directly onto the sample outer surface.

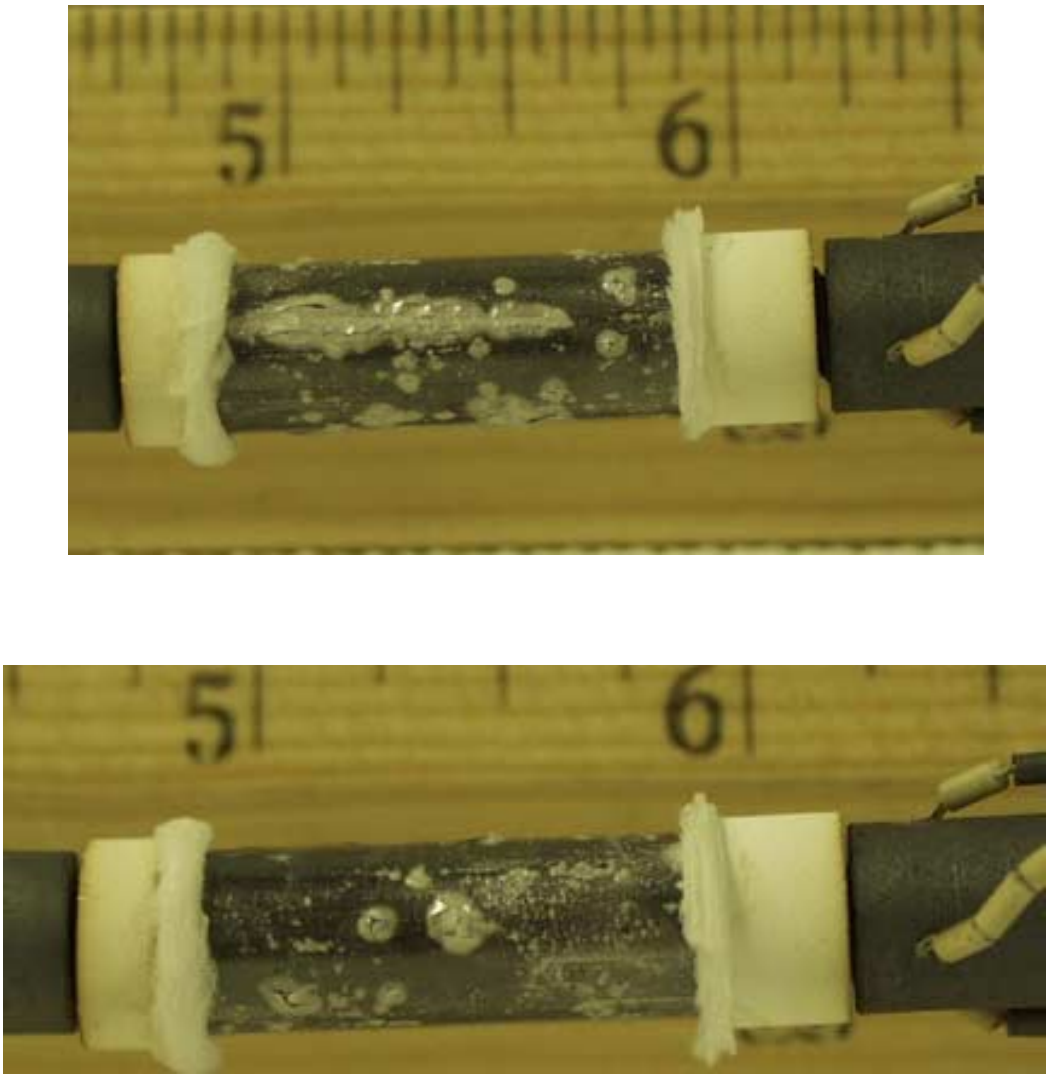

Fig. 5. Extensive monoclinic oxide formation, cracking and local breakaway oxidation observed for the as-received E110 EU#12 sample after 290 s at 1000°C (5% ECR).

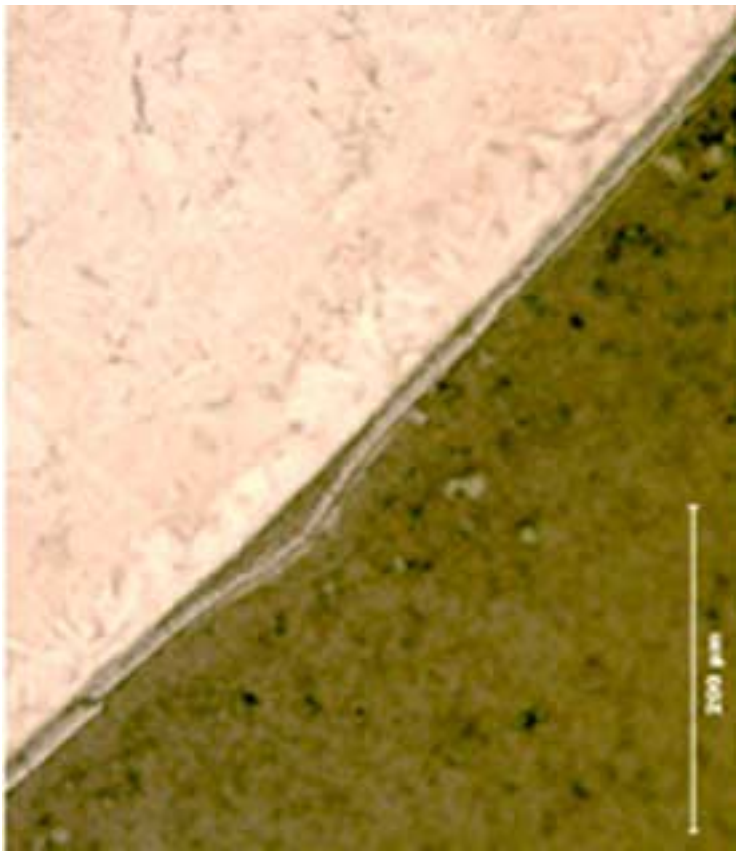

Fig. 6. Metallographic image of delaminated and cracked oxide on as-received E110 sample oxidized for a 290-s hold time at 1000°C. Sample is from Test EU#13.

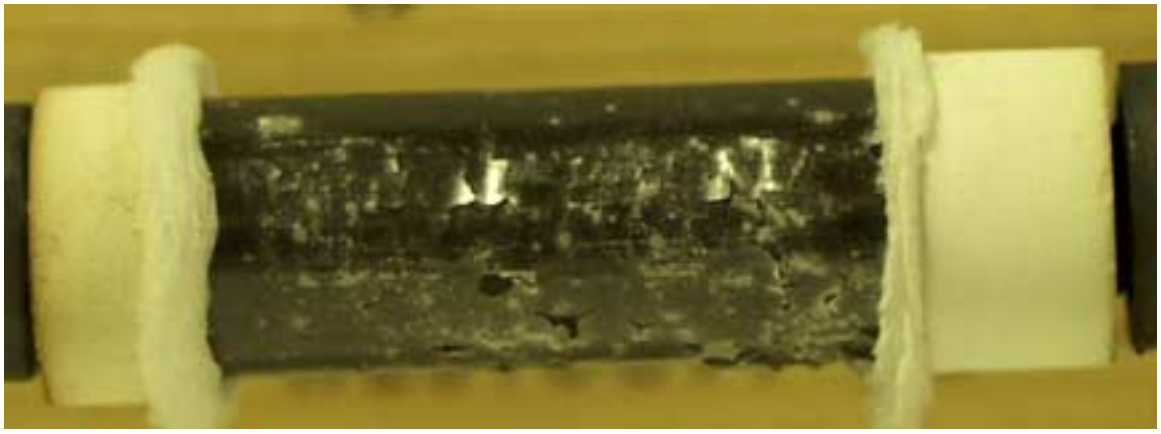

Fig. 7. Outer-surface oxide layer of EU#11 sample tested for a 290-s hold time at 950°C.

3.1.3 Results for Hold-times >290 s (EU#36, EU#38, EU#40, and EU#8)

Even before the 290-s hold-time tests were run, the EU#8 test was run for 1400 s at 1000°C in order to induce extreme breakaway oxidation and hydrogen uptake. As the measured hydrogen uptake (≈4200 wppm) was well beyond the amount needed for E110 embrittlement, test times between 290 s and 1400 s were explored to map the evolution of hydrogen uptake with time and calculated ECR. Although photographs of these samples were not taken, extensive hydrogen analyses were performed to determine the axial and circumferential variation of hydrogen uptake with time. It was interesting to observe that hydrogen uptake was locally high under regions of cracked white oxide and locally low under regions of uniform black oxide. This led to both circumferential and axial variations in hydrogen content. The results in Table 2 represent circumferentially averaged values, which are important for correlation with ring-compression test results.

After a 290-s hold time, the H-content at the center of the sample was 120±45 wppm, where the ±45 represents the one-sigma variation in readings from ≈4 arc segments. The variation is caused by the retention of hydrogen in the local area in which it entered the sample. It was surprising that the higher hold time of 395-s resulted in lower H-content than the 290-s sample. However, the evolution of breakaway oxidation is an instability phenomenon that may occur at different times from test-to-test and sample-to-sample. Local variation in surface roughness from sample-to-sample would be enough to cause such results, as well as possible hold-temperature differences of ±10°C around the circumference of the cladding. The lower H-content in the 395-s sample is consistent with the appearance of the outer-surface oxide for the EU#36 sample.

The 625-s hold-time showed high H-content and considerable variation. Based on circumferential averaging of the hydrogen-content measurements, the axial profile of hydrogen content is shown in Fig. 8. The measurements are consistent with physical observations, including the observation that the discontinuity at the ends of the sample is an initiation site for extensive monoclinic oxide formation and breakaway oxidation.

For the 825-s hold time sample, about half the sample experienced significant delamination and spallation, consistent with the H-content measurements of ≈540 wppm at the center and ≈1400 wppm in the delaminated/spalled off-center location. Complete delamination and spallation are shown in Fig. 9 for the 1400-s hold time sample.

The results of the hydrogen analyses are summarized in Figs. 10-11. In Fig. 10, the hydrogen content is plotted vs. hold time, while in Fig. 11 it is plotted vs. CP-model-predicted ECR. If we use the central location values from which ring compression samples would be cut, then we would expect embrittlement to occur in the range of 300-800 s, with corresponding CP-ECR values of ≈5-8%. Because of the end effects observed, samples <25 mm may have a lower transition time and ECR, while longer samples may have a higher transition time and ECR for embrittlement.

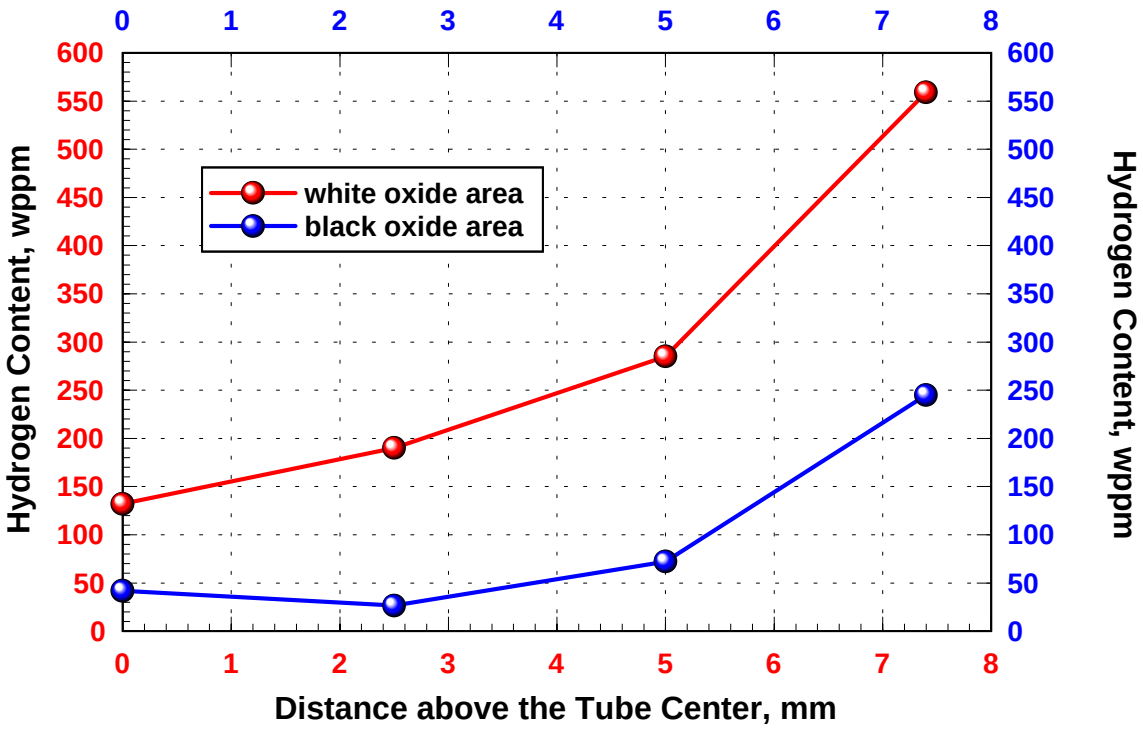

Fig. 8. Hydrogen content in E110 after oxidation Test EU#38 with as-received E110 exposed to steam at 1000°C for a hold time of 625 s (≈7% CP-model-predicted ECR).

Fig. 9. As-received E110 sample after two-sided steam oxidation for 1400 s (10% ECR) at 1000°C. Extensive monoclinic oxide formation, breakaway oxidation, delamination and spallation are observed. The measured hydrogen content is 4230 wppm.

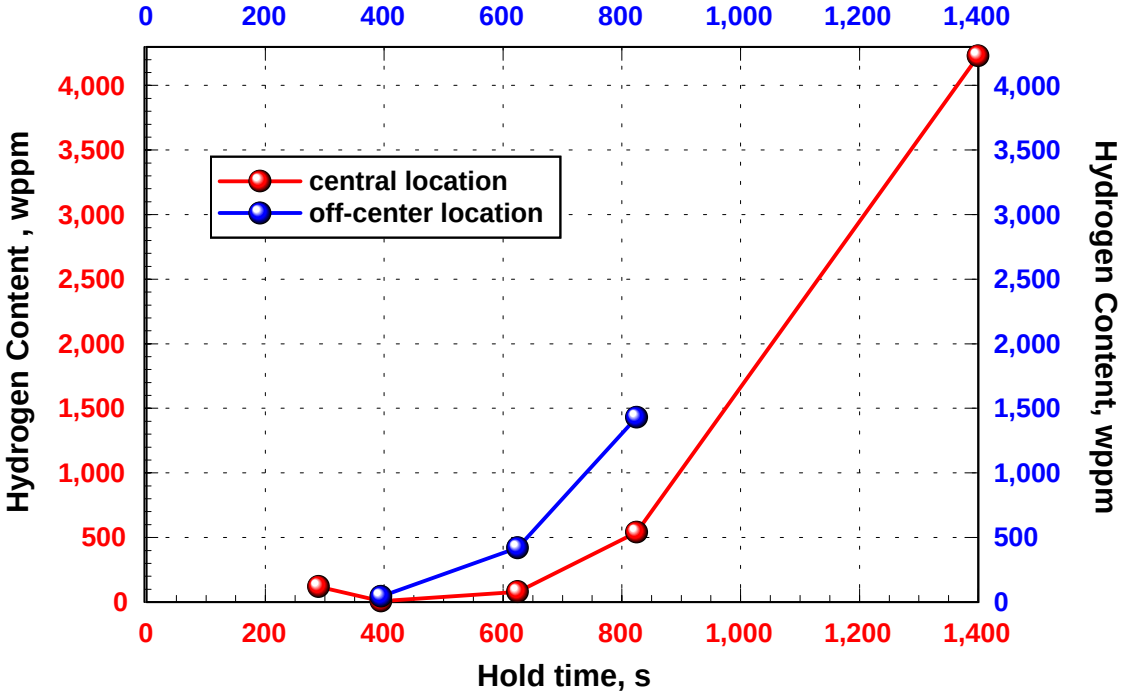

Fig. 10. H-content vs. hold time for as-received E110 after two-side oxidation tests at 1000°C.

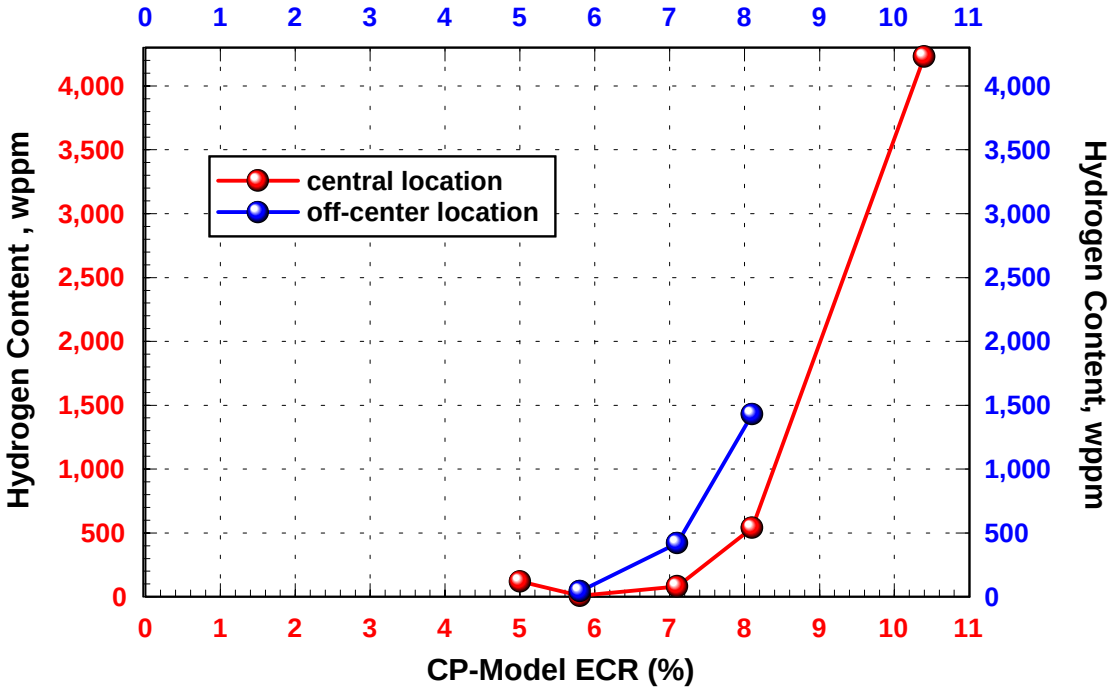

Fig. 11. H-content vs. ECR for as-received E110 after two-side oxidation tests at 1000°C.

3.1 Results of One-sided Steam Oxidation Tests Conducted at 1100°C

Prior to conducting the two-sided oxidation tests at 1000°C, several one-sided tests were conducted at 1100°C in order to evaluate the nature of the oxide layer formed and the hydrogen uptake. The intent was not to develop an extensive database at 1100°C, as RRC-KI/RIAR has already done that and reported their results at NSRC-2002. Rather the purpose was to investigate the evolution of the nodular breakaway oxidation and embrittlement observed by RRC-KI/RIAR investigators. Fast-ramp-rate control parameters were used for these tests, so that the hold time at 1100°C essentially represents the total time from ramp initiation at 300°C to test completion at 1100°C. Table 3 summarizes the test conditions and results for these tests.

Table 3 Summary of One-Sided, Steam Oxidation Test Results at 1100°C on As-Received E110; Δw_o is the surface-area-normalized weight gain due to oxygen pickup; Test EU#2A was conducted with an etched-and-anodized sample; measured weight gains are not reliable because of partial inner-surface oxidation near sample ends and flaking off of monoclinic oxide from the outer surface

Test ID	Hold Time s	CP ECR %	CP Δw_o mg/cm^2	Meas. Δw_o mg/cm^2	H-Content wppm	Comment
EU#3	200	3.6	5.6	5.3	---	White spots observed at high mag.
EU#2	512	5.8	9.0	9.0	---	Visible white spots (Fig. 12a)
EU#2A	512	5.8	9.0	8.2	---	Visible white spots (anodized sample)
EU#1	1400	9.6	14.9	14.1	---	Visible white spots (Fig. 12b)
EU#4	2473	11.8	18.3	24.0	182	Regions of cracked white oxide (Fig. 13a) and pronounced nodes (Fig. 13b)
EU#5	3800	15.8	24.6	37.5	204	Larger regions of cracked white oxide (Fig. 14)

Similar to the early-time results observed after oxidation at 1000°C, white spots of presumed monoclinic oxide are observed in a matrix of black tetragonal oxide (EU#3). After 512 s (Fig. 12a) and 1400 s (Fig. 12b) in steam at 1100°C, the white-grey areas are clearly visible. However, unlike the 1000°C results for this hold-time range, the spots remain essentially isolated and are more stable in the black matrix. After ≈2500 s in steam at 1100°C, the white spots grow, crack and partially connect on the surface of the sample (Fig. 13a) and the oxide nodes grow deeply into the metal (Fig. 13b). After 3800 s, more extensive cracking and

interconnection occur (Fig. 14). However, the hydrogen content does not exceed ≈200 wppm at this exposure time, even though the appearance of the surface would suggest otherwise.

It appears that nodular oxidation is dominant at 1100°C and the nodes are much more stable than they are at 1000°C. Local breakaway oxidation occurs due to cracking through the node thickness direction. Cracking all the way to the base metal may explain the hydrogen uptake, but it is clearly limited at 1100°C. One possible explanation for the differences observed is that the monoclinic-to-tetragonal oxide phase transition for stress-free, stoichiometric ZrO_2 is ≈1120-1140°C – difficult to measure because it is difficult to grow a stress-free stoichiometric oxide on Zr. Thus, although the 1100°C results clearly show a mixture of oxide phases, the tetragonal phase tends to be more stable closer to the transition temperature.

(a)

(b)

Fig. 12. Visible regions of isolated white spots – presumed to be monoclinic oxide nodes – after one-sided steam oxidation of as-received E110 at 1100°C after (a) 512 s and (b) 1400 s.

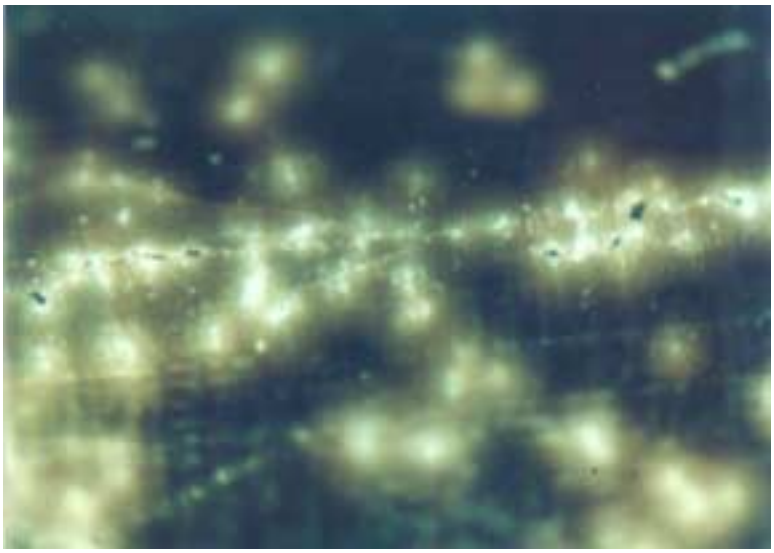

(a)

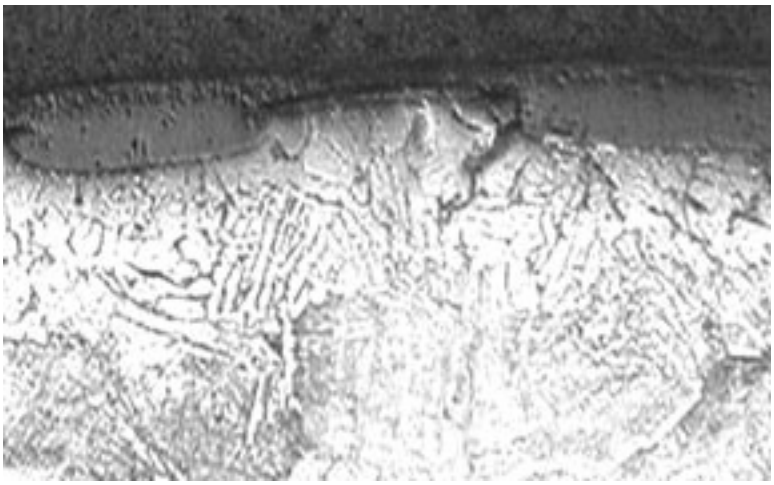

(b)

Fig. 13. Some interconnection of white monoclinic oxide spots (a) observed on the surface and high-magnification (100x) of growth of these white nodes (b) into the oxygen-stabilized alpha layer of as-received E110 after 2473 s of one-sided oxidation at 1100°C. Hydrogen concentration is 182 wppm, indicating crack extension to base metal during oxidation.

(a)

(b)

Fig. 14. Low (a) and high (b) magnification of the surface of as-received E110 after one-sided steam oxidation at 1100°C for 3800 s. Regions of high interconnection of monoclinic oxide nodes and more significant cracking within these interconnected regions are observed. Hydrogen concentration is 204 wppm, indicating crack extension to the base metal during oxidation.

4. Test Results for Polished and Machined-and-Polished E110 Sample

Because the high surface roughness of as-received E110, as well as the surface/substrate chemistry, could contribute to the early formation of monoclinic oxide followed by local (1100°C) and/or global (1000°C) breakaway oxidation, a series of experiments were performed with polished and machined and polished samples. The results were very encouraging in that breakaway oxidation was delayed for the polished and machined-and-polished (M-P) E110 surfaces. Additional tests were then performed to determine the weight gain kinetics of E110 vs. M5 for time periods during which the oxide layer remained intact. At 1000°C, these times were extended to determine the hydrogen concentration vs. time and ECR.

4.1 Results of Polished and Machined-and-Polished E110 Samples Oxidized at 1000°C

In Test EU#13 (1000°C for 290 s to 5% ECR), half of the sample was in the as-received condition and half the sample was machined on the outer surface (38 μm removed) and polished. Based on visual and low-magnification inspection (Fig. 15), the oxide on the machined-polished segment appears uniform and lustrous-black, while the non-treated segment shows the mix of white (monoclinic oxide) regions in a matrix of black (tetragonal) oxide observed in the other tests with as-received E110. Metallography was performed to confirm that the black oxide layer on the M-P of the sample was indeed intact (Fig. 16a), while the oxide on the as-received part of the sample was cracked and partially delaminated (Fig. 16b).

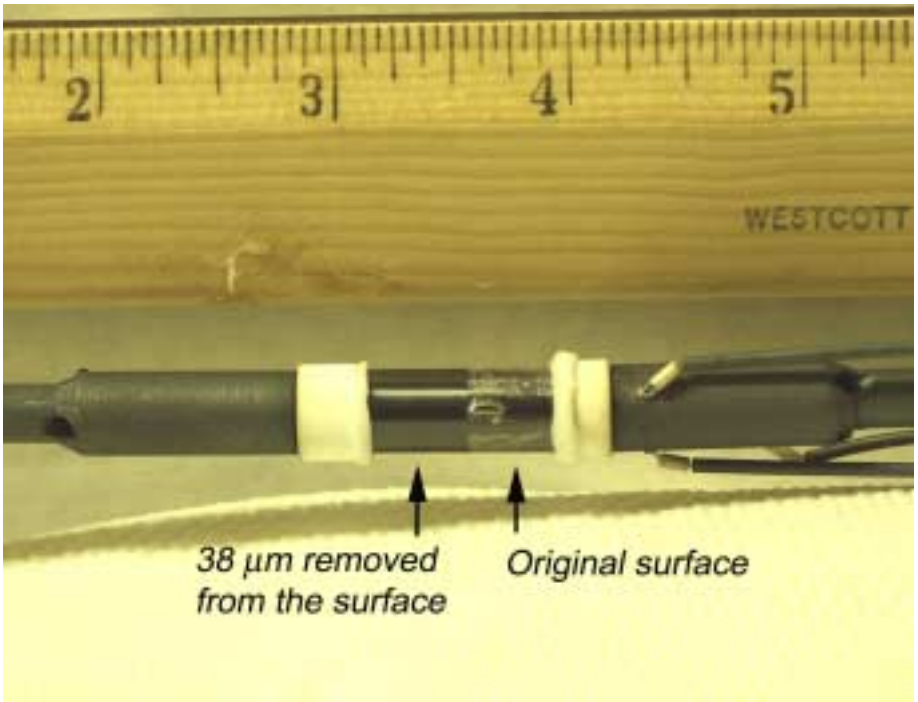

Fig. 15. Superior performance of machined-and-polished E110 outer surface oxidation compared to as-received material at 1000°C for 290 s (5% ECR). A smooth black (tetragonal) oxide is observed to form on the machined-and-polished surface.

(a)

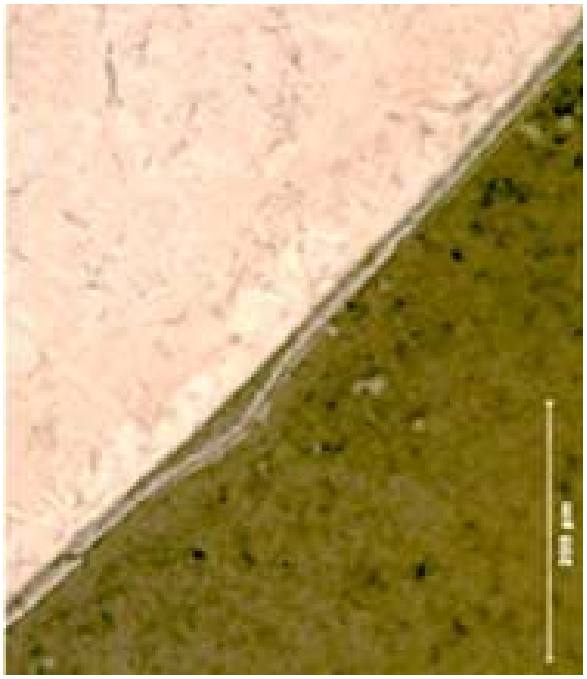

(b)

Fig. 16. Metallographic images of (a) intact oxide layer on machined-and-polished E110 surface and (b) cracked/delaminated oxide layer on as-received E110 surface following two-sided steam oxidation at 1000°C for 290 s. Scale bar is 200 μm.

Test EU#14 was run to determine the relative benefits of polishing vs. machining-polishing on the steam oxidation performance of E110 at 1000°C and 5% ECR. As shown in Fig. 17, the sample consisted of three axial regions: A) machined (25 μm removed) and polished; B) polished only; and C) as-received.

Figure 18 shows that both the polished-only and the machined-and-polished sample preparations resulted in a smooth, black oxide formation on the outer surface in contrast to the behavior of the as-received region. From the low-magnification photograph in Fig. 18, it appears that polishing alone is sufficient to improve the behavior of E110. Polishing smoothes out the surface roughness by removing a few microns from the surface. In the process, chemical impurities and alloy constituents near the surface are also removed.

To further investigate the effects of polishing and machining-polishing, higher (200x) magnification photographs were taken of the surfaces of the three regions of the EU#14 sample. Figure 19a shows the machined-and-polished outer surface after oxidation with very small (≤25 μm), isolated spots of monoclinic oxide. Figure 19b shows the same magnification of the polished outer surface after oxidation with slightly larger (≤75 μm) spots of monoclinic oxide. Figure 19c shows the outer surface of the as-received material after oxidation with large regions of monoclinic (light-colored) oxide.

It is clear that the quality of the oxide layer on the polished surface is much better than the as-received surface. This suggests that the oxidation behavior of the E110 alloy is sensitive to some combination of surface roughness and surface chemistry. The performance was improved somewhat more by the combination of the removal of 25 μm from the outer surface and polishing of the machined surface. Thus, further improvement may be achieved by removing some of the near-surface layer, as well as the surface itself. It is also worth noting that the untreated inner surface of the sample exhibited large regions of monoclinic oxide visible at low magnification. However, neither treatment eliminated the initiation of monoclinic oxide spots, although both treatments slowed down the initiation and growth of the monoclinic regions and may have decreased significantly the number density of initiation sites.

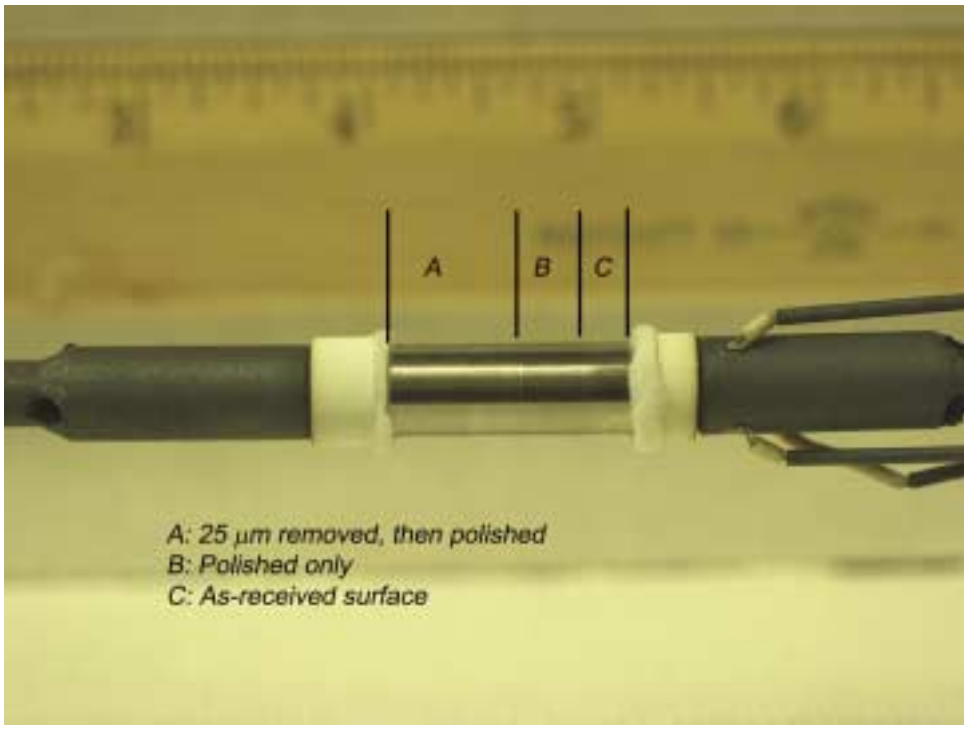

Fig. 17. E110 sample before oxidation test EU#14 at 1000°C for 290s (5% ECR).

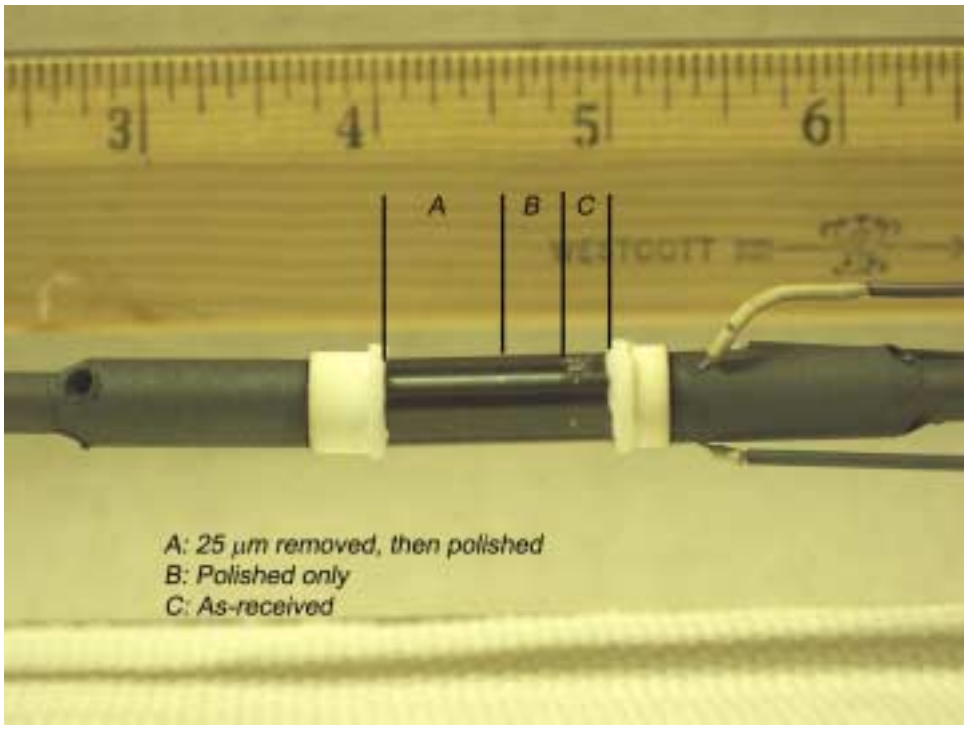

Fig. 18. E110 sample after test EU#14 steam oxidation at 1000°C for 290 s (5% ECR).

(a)

(b)

(c)

Fig. 19. High-magnification images of the of the steam-oxidized (1000°C for 290 s) surfaces of (a) machined-and-polished E110, (b) polished E110 and (c) as-received E110.

Test EU#16 was run to determine if outer and inner surface polishing would be sufficient to achieve ≈10% calculated ECR at 1000°C without breakaway oxidation. As shown in Fig. 20, extensive formation of monoclinic oxide is evident on one side of the sample. Spallation and delamination of this oxide was observed during the cooling phase of the test. The remaining oxide surface underneath this spalled region is dull-black and rough in appearance. This is also what is observed on the surface of other cladding alloys (e.g., Zry-4 and M5) after classical breakaway oxidation. However, about half the outer surface still consists of black tetragonal oxide, which experienced no apparent delamination or spallation. Figure 21 shows a high magnification micrograph of this region, with no evidence of monoclinic oxide formation. This is in dramatic contrast to the behavior of the as-received cladding (Fig. 9) under similar test conditions.

The sample for Test EU#17 was machined-and-polished on the inner and outer surfaces and tested at the same temperature as EU#16, but for longer time (1325 s vs. 1025 s). As shown in Fig. 22, the extent of monoclinic oxide formation, cracking and spallation is as significant as for the polished-only EU#16 sample. As the oxidation furnace has a viewing window port, the observations vs. time of the experimenter are very interesting: (a) att 325 s (4.3% ECR) into hold time at 1000°C, white spots observed on outer surface; (b) outer-surface oxide looks good from 325 to <1100 s (9% ECR); (c) breakaway oxidation initiates at ≈1100 s (9.4% ECR) at 1000°C; and (d) extensive breakaway oxidation is observed at 1175 s (9.7% ECR) at 1000°C.

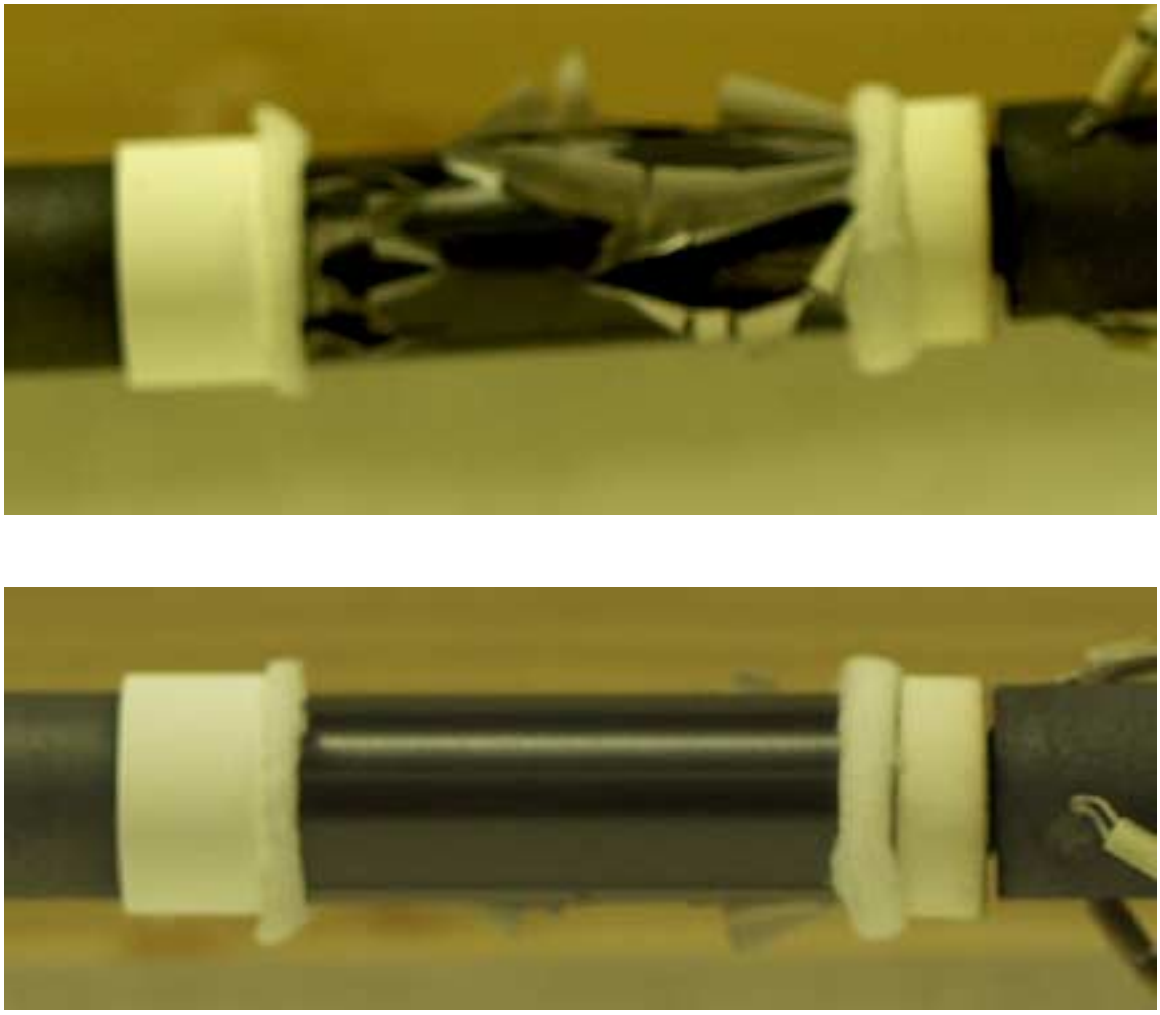

Fig. 20. Inner-and-outer-surface polished EU#16 E110 sample after 1025 s (≈9% ECR) in steam at 1000°C. Extensive monoclinic oxide formation, delamination and spallation is evident on one side of the sample, while the other side remains intact.

Fig. 21. High magnification (200x) micrograph of the shiny-black region of the EU#16 E110 outer surface after 1025 s (≈9% ECR) in steam at 1000°C. The region is relatively free of monoclinic oxide formation.

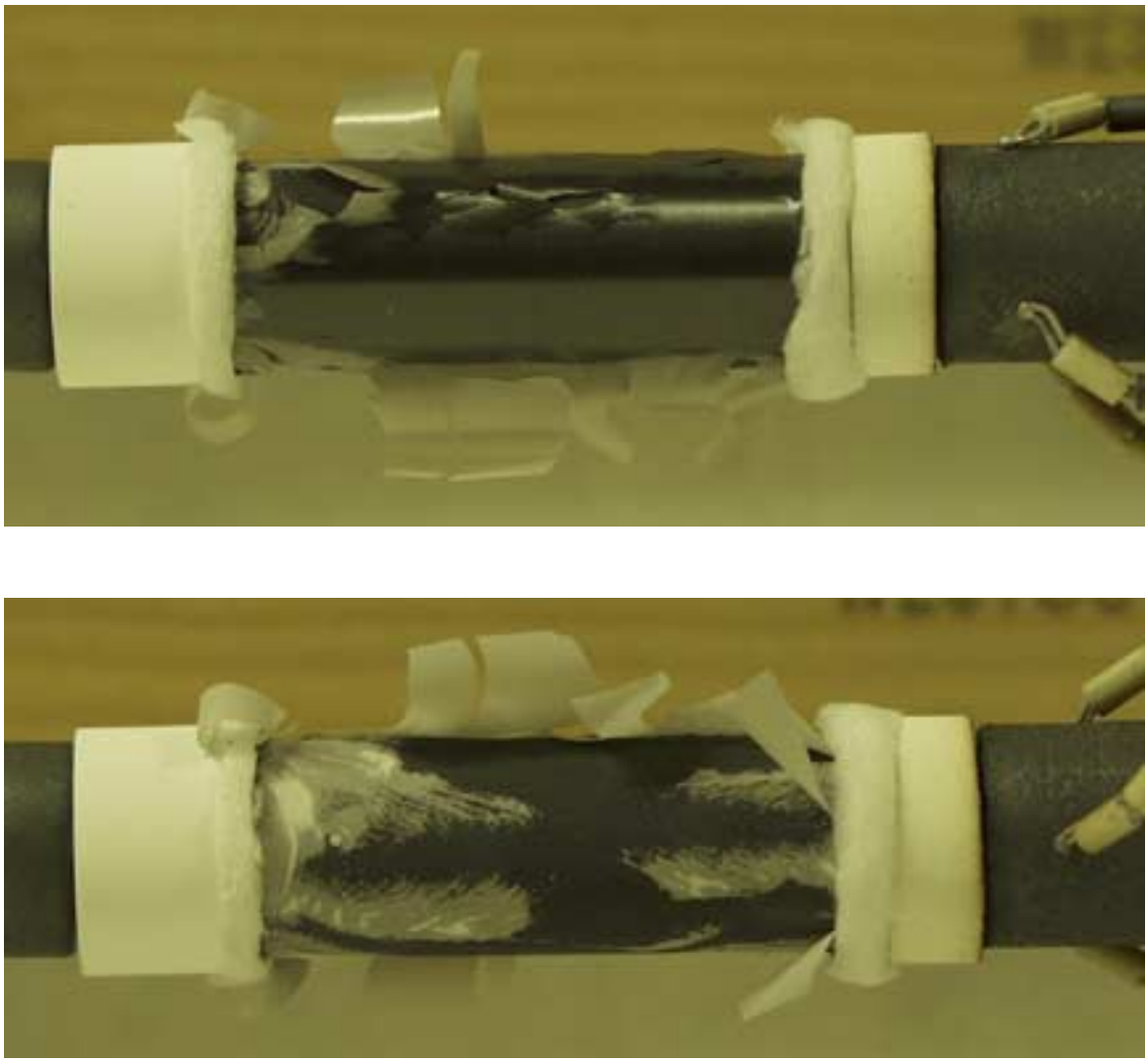

Fig. 22. Machined-and-polished (inner and outer surface) EU#17 E110 sample after 1325 s (≈10% ECR) in steam at 1000°C. Extensive monoclinic oxide formation, delamination and spallation are evident over some of the cladding outer surface. The oxide under the spalled region is dull-black and rough in appearance.

In order to better understand the differences between E110 and M5 during steam oxidation, it is important to test both materials under the same conditions. Because E110 has a thicker wall (0.71 mm vs. 0.57-0.61 mm for M5), its thermal response is slower than that of M5 in the ANL Oxidation Apparatus during the temperature ramp from 300°C to 1000°C. In order to ensure that E110 and M5 samples experience the similar temperature histories, ≈115 μm was machined from the E110 inner surface and both inner and outer surfaces were polished. This results in equivalence between the thermal masses and thermal responses of E110 and M5, as well as an E110 wall thickness (0.60 mm) close to that of M5 (0.57-0.61 mm). Based on the M5 thermal benchmark tests, the sample temperature history for the 1000°C hold temperature is given in Fig. 23 (≈70°C/s temperature ramp from 300-900°C and ≈1.4°C/s ramp from 900-1000°C; elapsed time from start of ramp to hold temperature is ≈89 s).

Results for the E110 tests (EU#19-27) are recorded in Table 4. The samples exhibit uniform black oxide layers at low magnification up to hold times of ≈240-290 s. The weight gains (normalized to surface area) for samples that exhibit uniform black oxide on the outer surface are recorded in Table 4. Consistent with previously published results for M5, these weight gains at 1000°C are less than those predicted by the Cathcart-Pawel model (see Fig. 24). The weight gain coefficient k (in $mg/cm^2/s^{0.5}$) at 1000°C, for $\Delta w = k\ t^{0.5}$, is: 0.2242 for the Cathcart-Pawel model, 0.162 for polished E110 (excluding data points for EU#22-23), 0.132 for as-received M5 and 0.109 for the M5 tested in the French CINOG experiments. The ANL values were determined through best linear fit for k^2 from $(\Delta w)^2 - (\Delta w_r)^2 = k^2\ t_s$, where $\Delta w_r = 1.5$ mg/cm^2 is the weight gain during the temperature ramp. Thus, the oxidation behavior of E110 is essentially the same as that of M5 at 1000°C for test times during which the E110 oxide layer remains tetragonal (uniform and lustrous black).

Additional tests were performed with polished and machined-and-polished E110 to determine the time at 1000°C at which the hydrogen content increases dramatically. It is assumed that this hydrogen increase will correlate with the transition from ductile to brittle behavior. The test matrix and results for this series of tests are shown in Table 5. The hydrogen content vs. time is shown in Fig. 25, while the hydrogen content vs. CP-predicted ECR is shown in Fig. 26. Given the axial and circumferential variation of hydrogen content, there may be a lot of scatter in the correlation between total hydrogen content for a ring and embrittlement.

Table 4 Two-Sided Oxidation Tests Conducted on Modified E110 Cladding at 1000°C; polished cladding outer diameter is 9.17 mm; machined and polished inner diameter is 7.98 mm and wall thickness is 0.6 mm; T_s = sample hold temperature, t_s = hold time at T_s, Δw_p = predicted normalized weight gain based on Cathcart-Pawel correlation; Δw_m = measured normalized weight gain based on sample weight change; ECR = 1.235 Δw is referenced to the as-received E110 wall-thickness of 0.71 mm

Test ID#	t_s s	Pred. ECR %	Pred. Δw_p mg/cm^2	Meas. Δw_m mg/cm^2	H Content wppm	Outer-Surface Oxide
EU#25	0	1.8	1.5	1.5	---	Lustrous Black
EU#19	41	2.6	2.1	1.9	---	Lustrous Black
EU#20	106	3.3	2.7	2.3	---	Lustrous Black
EU#21	190	4.2	3.4	2.7	---	Lustrous Black
EU#22	292	5.2	4.2	3.1	---	Lustrous Black
EU#23	413	5.9	4.8	>3.4	---	Lustrous Black with white Spots at 236 s
EU#24	413	5.9	4.8	>3.1	11±5	Lustrous Black with white Spots at 281 s
EU#26	413	5.9	4.8	>2.9	---	Lustrous Black with white end regions
EU#27	413	5.9	4.8	>3.0	--	Lustrous Black with white end regions

Table 5 Two-Sided Oxidation Tests Conducted on Polished and Machined-and-Polished E110 Cladding at 1000°C; polished cladding outer diameter is 9.17 mm; t_s = hold time at 1000°C, Δw_p = predicted normalized weight gain based on Cathcart-Pawel correlation; ECR = 1.235 Δw is referenced to the as-received E110 wall-thickness of 0.71 μm

Test ID#	t_s s	Pred. ECR %	Pred. Δw_p mg/cm^2	H Content wppm	Outer-Surface Oxide
EU#22	292	5.2	4.2	---	Lustrous Black
EU#24	413	5.9	4.8	11±5	Lustrous Black with white ends
EU#37	815	8.1	6.6	6±1	---
EU#16	1025	9.1	7.4	150 (32-342)	See Fig. 20 for variation in outer surface oxide layer
EU#41	2025	12.5	10.1	1280±100	---

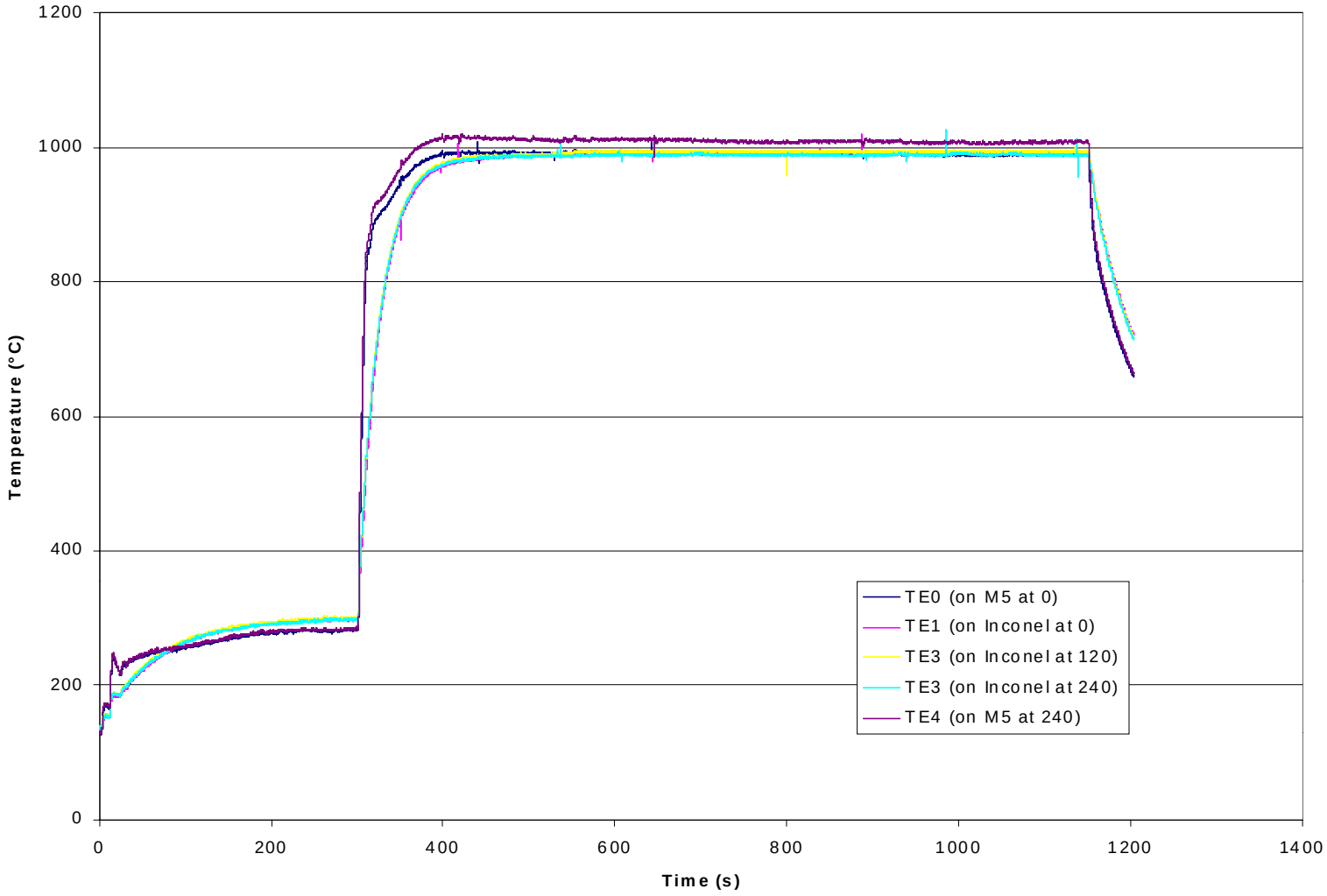

Fig. 23. Thermal benchmark results for M5 sample (MU#22) for a hold temperature of 1000°C.

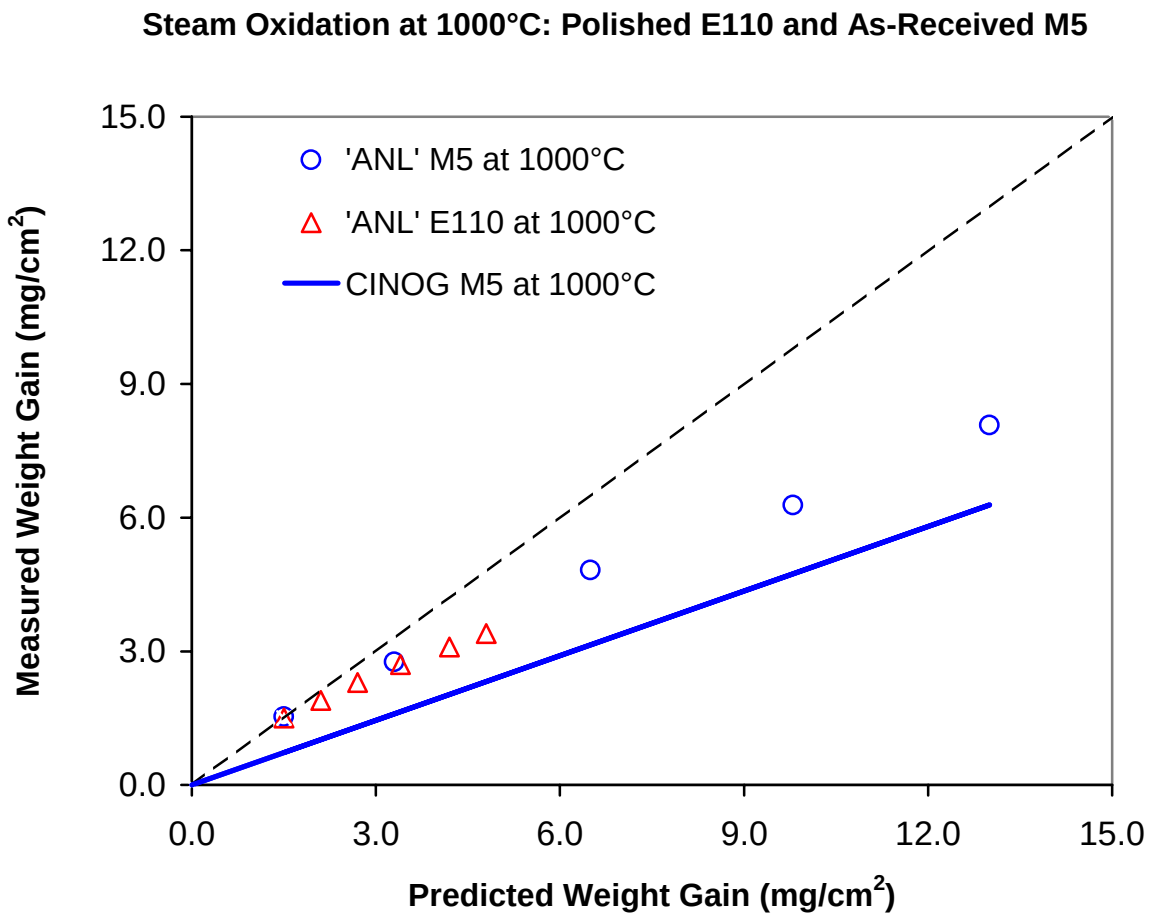

Fig. 24. Comparison of measured vs. predicted weight gain from steam oxidation at 1000°C for machined-and-polished E110 tested at ANL, as-received M5 tested at ANL and, and M5 tested in the CINOG experiments in France. Predicted values are based on the integration of the Cathcart-Pawel rate equation over the sample temperature profile shown in Fig. 23.

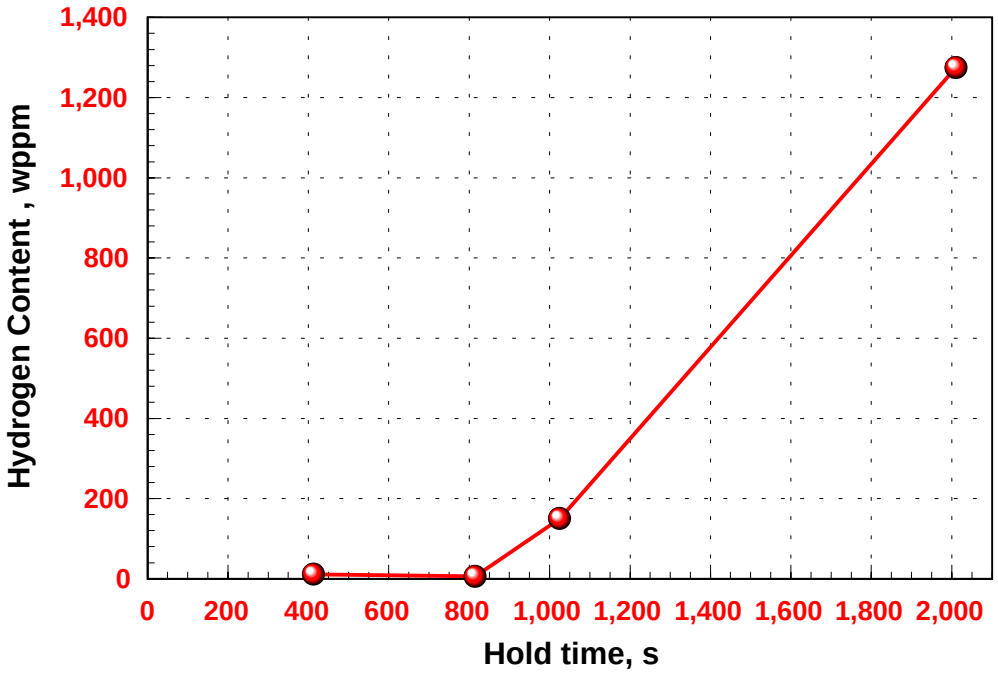

Fig. 25. Increase in hydrogen content with hold time at 1000°C for polished and machined-and-polished E110 samples oxidized in steam.

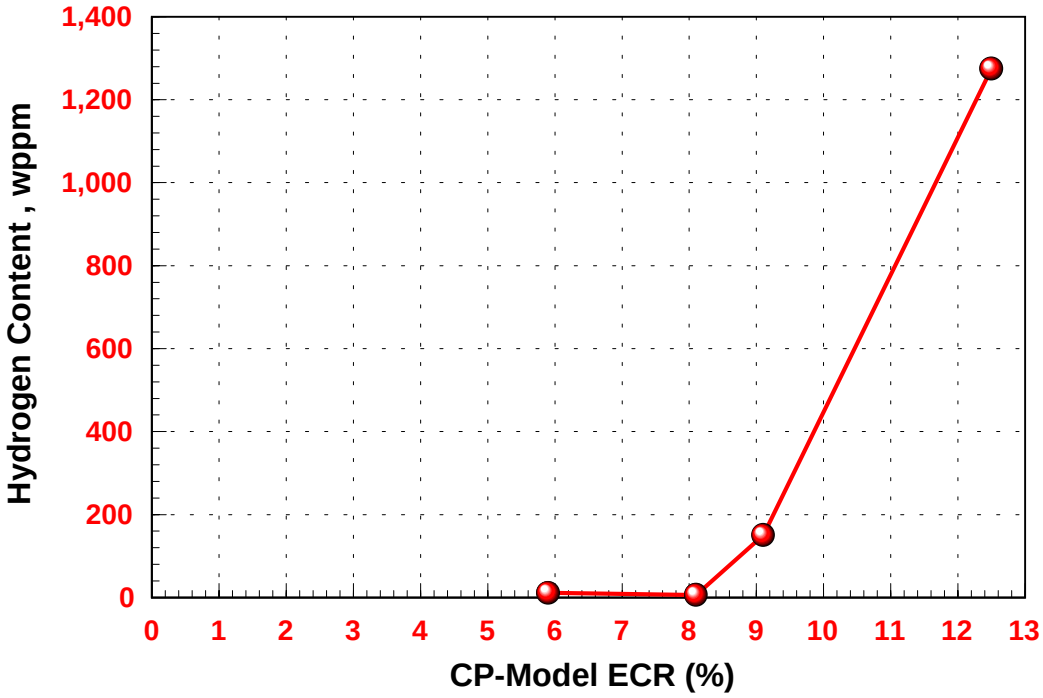

Fig. 26. Increase in hydrogen content with Cathcart-Pawel-predicted ECR at 1000°C for polished and machined-and-polished E110 samples oxidized in steam.

4.2 Results of Polished and Machined-and-Polished E110 Samples Oxidized at 1100°C

A series of tests were conducted with machined (to 0.6-mm wall thickness) and polished E110 samples to determine weight gain kinetics prior to breakaway oxidation for comparison to the Russian alloy G110, which also exhibits good oxidation behavior, and to M5. Table 6 shows the test conditions and results. All samples exhibited a lustrous black oxide layer up to the highest test time of 1011 s. At this test time, small white spots were observed on the outer surface oxide layer. The temperature history for the 1100°C oxidation tests with M5 wall-thickness is shown in Fig. 27. The weight gain results are plotted in Fig. 28 vs. the CP-predicted weight gain. Unlike the results at 1000°C, much better agreement is achieved between the E110 weight gain kinetics and the CP-predicted values. Similar behavior is observed for the M5 tested at ANL. The ANL results are also in good agreement with the G110 alloy tested by RRC KI.

Table 6 Summary of Two-Sided Oxidation Test Results at 1100°C for Machined-and-Polished Samples; polished cladding outer diameter is 9.17 mm; machined-and-polished inner diameter is 7.98 mm and wall thickness is 0.6 mm; Δw_p = predicted normalized weight gain based on Cathcart-Pawel correlation; Δw_m = measured normalized weight gain based sample weight gain; ECR = 1.235 Δw is referenced to the as-received E110 wall-thickness of 0.71 mm

Test ID	Hold Time s	CP ECR %	CP Δw_p mg/cm^3	Meas. Δw_m mg/cm^3	Comment
EU#29	111	6.4	5.2	4.8	Lustrous black oxide
EU#31	361	10.3	8.3	7.1	Lustrous black oxide
EU#32	511	11.7	9.5	8.4	Lustrous black oxide
EU#30	576	12.5	10.1	---	Lustrous black oxide
EU#33	1011	15.9	12.9	10.6	Lustrous black oxide with small white spots

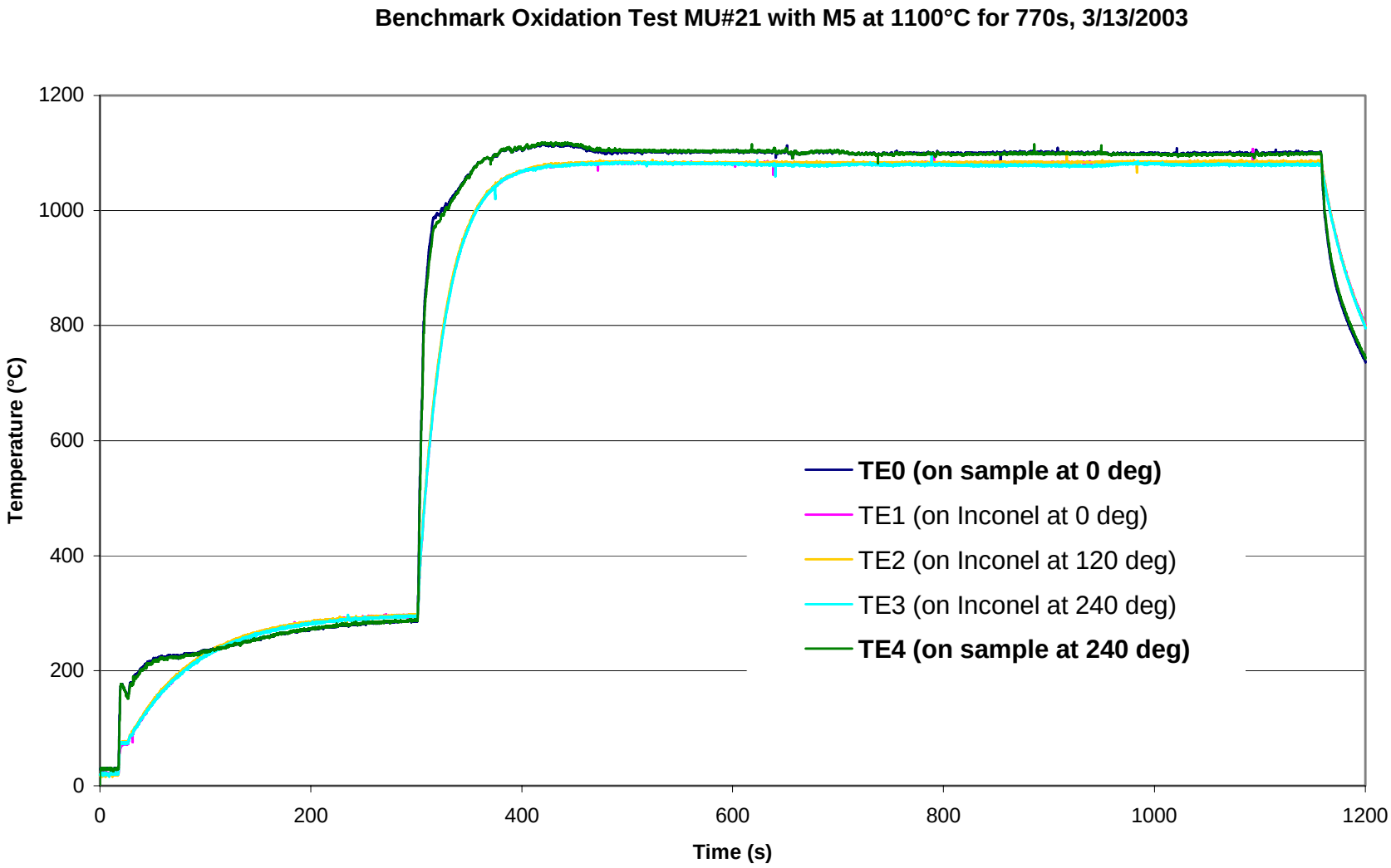

Fig. 27. Thermal benchmark results for M5 sample (MU#21) for a hold temperature of 1100°C.

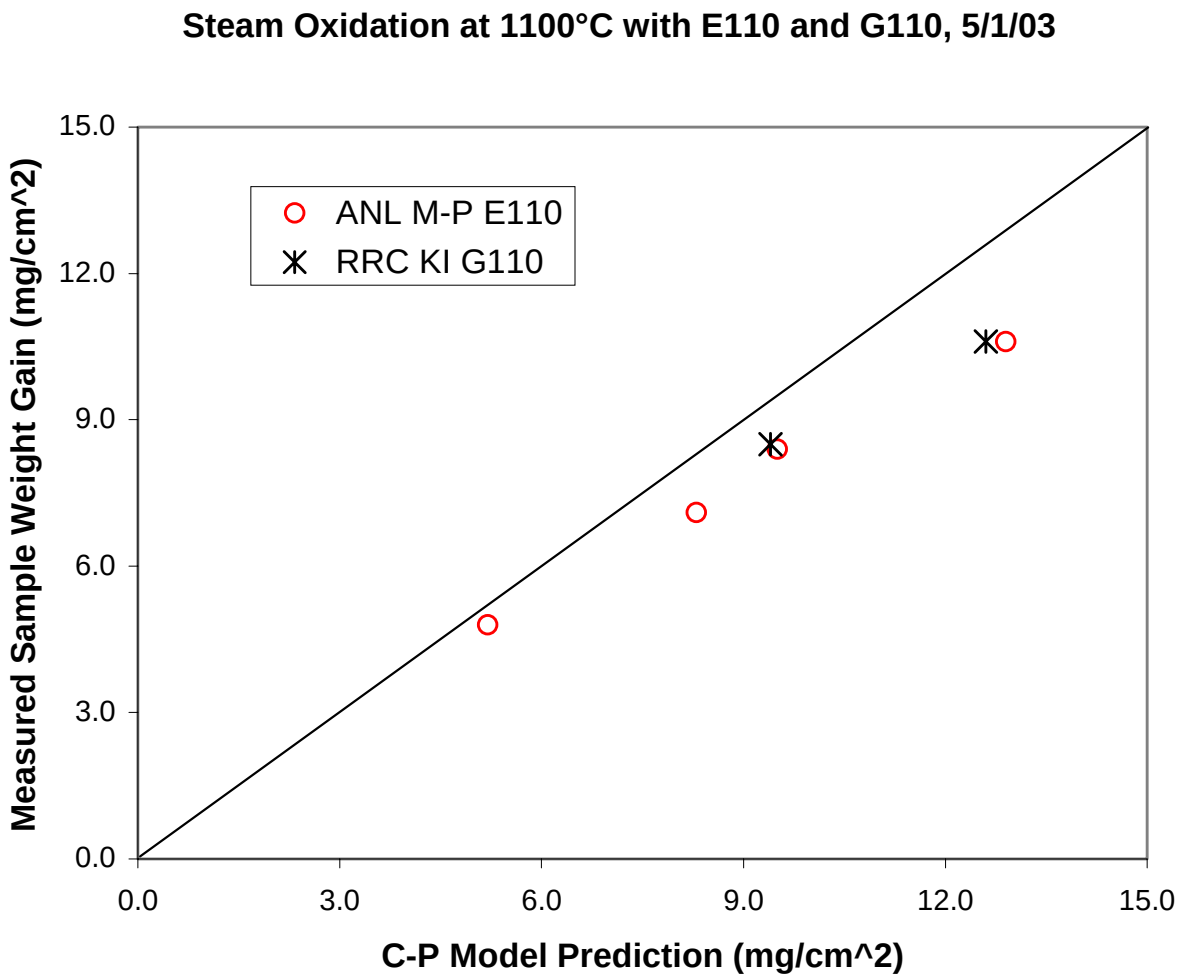

Fig. 28. Comparison of ANL weight gain results for machined-and-polished E110 samples with RRC KI results for Alloy G110 and the Cathcart-Pawel (C-P) model predictions for steam oxidation at 1100°C.

5. Effects of Pre-Etching on E110 Steam Oxidation Behavior at 1000°C

A series of experiments were performed to determine the effects of etching on the steam oxidation behavior of E110 at 1000°C. All tests were conducted for a hold time of 290 s, which corresponds to a CP-model-predicted ECR = 5%. Etching tends to remove surface oxides and impurities, as well as to smooth out the surface roughness. However, HF is generally used as part of the etching solution to remove the oxide film on zirconium alloys. Depending on the strength of the HF in the solution, the etching time, the roughness of the surface, and the surface/substrate chemistry and microstructure, a significant amount of fluorine – which is known to enhance monoclinic oxide formation – may be adsorbed onto the surface and absorbed up to <1 μm into the substrate.

Figures 29-30 show the results of experiments with various etchants used on as-received E110, on surfaces that were polished after etching and on surfaces that were polished prior to etching. The test results indicate that the rough (≈0.35 μm) outer surface of E110 exhibits extensive monoclinic oxide formation, that polishing after etching restores E110 and negates the effects of F pickup, but that etching a polished E110 surface results in much poorer performance in steam at 1000°C than all the other alloys tested under the same conditions. The results for the polished E110 surface with a roughness of ≈0.13 μm are very interesting. This value of roughness is comparable to the outer-surface roughness of the other alloys (M5, Zry-4 and ZIRLO) tested. However, following pre-etching, polished E110 shows a much more dramatic response to steam oxidation at 1000°C for 290 s than the other alloys show after 2400 s in steam at 1000°C.

In summary, pre-etched E110 exhibits extensive surface overage of monoclinic oxide following steam oxidation. Polishing the pre-etched surface before steam oxidation restores the material to the good level of performance exhibited by polished (without pre-etching) E110. However, pre-etching polished E110 results in more extensive outer-surface monoclinic oxide formation than exhibited by the other alloys with similar surface roughness and pre-etched under the same conditions.

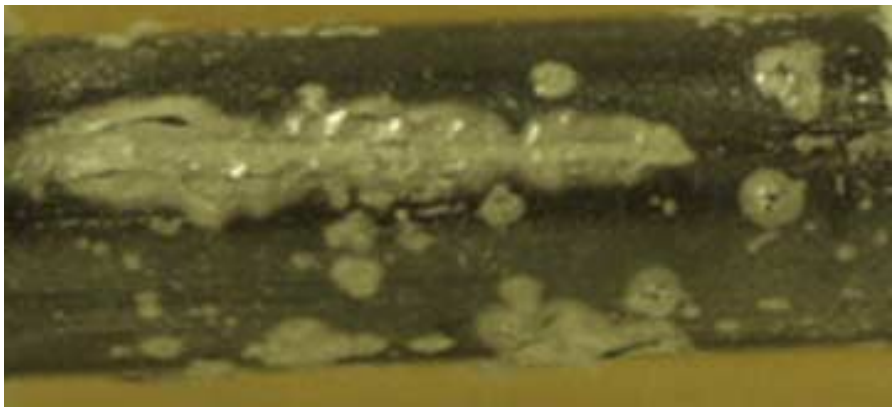

(a) as-received

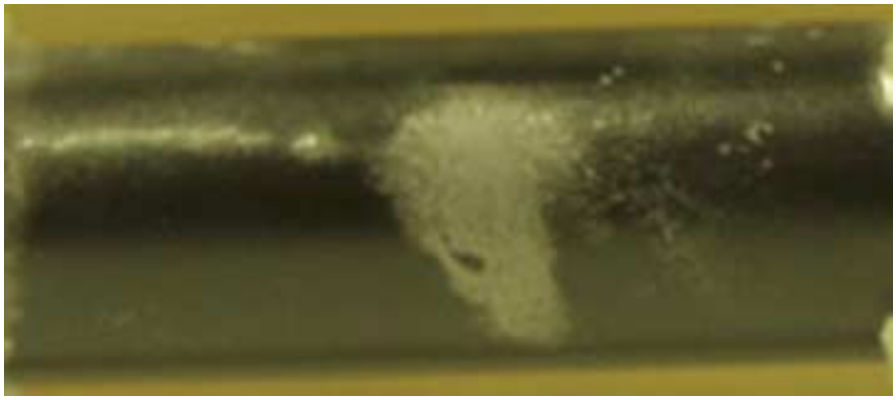

(b) etched with old solution

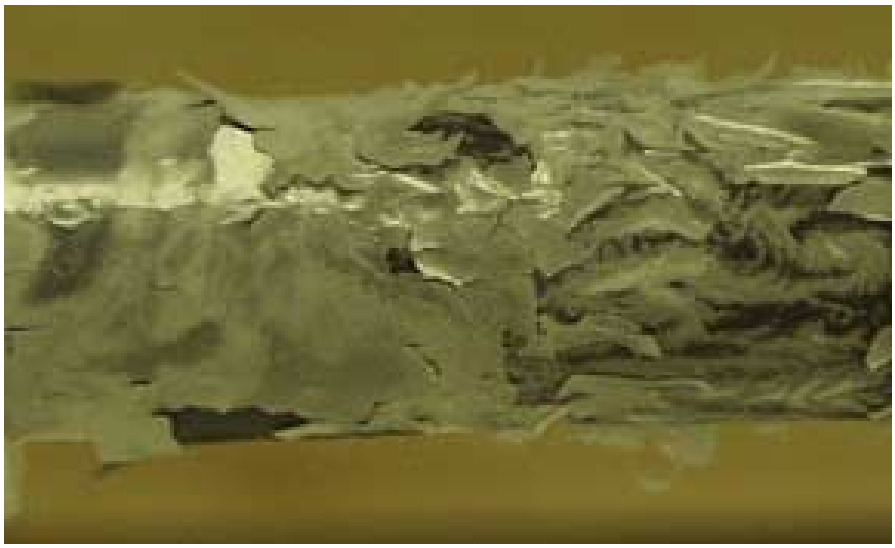

(c) etched with fresh solution

Fig. 29. Oxide surfaces on E110 tubing after steam oxidation at 1000C for ≈290 s (5% calculated ECR): (a) as-received tubing; (b) etched with old solution for 30 s; and (c) etched with fresh solution (25 ml HF + 25 ml HNO_3 + 75 ml $C_3H_6O_3$ + 62 ml H_2O) for 30 s.

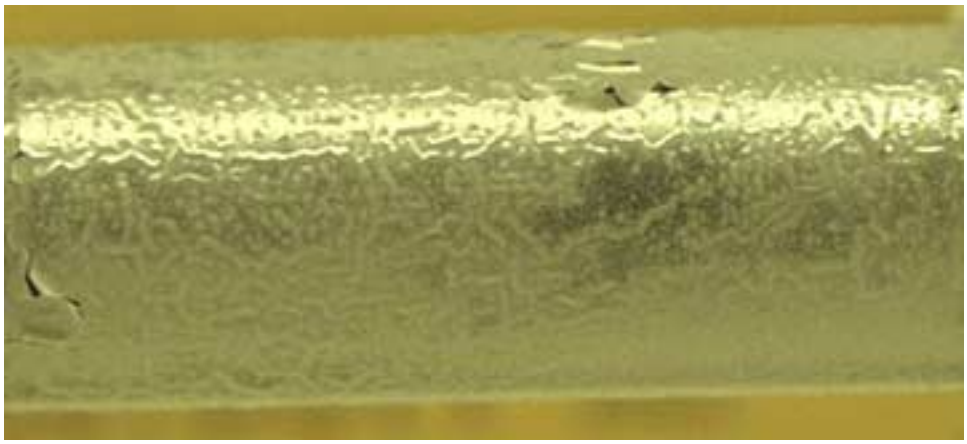

(a)

(b)

(c)

Fig. 30. Oxide surfaces on E110 tubing after steam oxidation at 1000C for ≈290 s (5% calculated ECR): (a) etched with standard etchant for Zry-2 (3.5 ml HF + 45 ml HNO_3 + 51.5 ml H_2O for 3 minutes); (b) etched with standard Zry-2 solution and outer-surface polished (note: unpolished inner surface is white), and c) polished-and-etched with standard solution for Zry-2.

6. Preliminary Conclusions

6.1 As-received E110 Tubing

The E110 tubing tested at ANL shows a high degree of susceptibility to nodular oxidation and breakaway oxidation at relatively low test times in steam at 1000-1100°C, as compared to other alloys tested under the same conditions. Although the initiation of the nodes – presumed to be mostly monoclinic oxide – is similar for 1000-1100°C test temperatures, their evolution is highly temperature dependent. At 1100°C, the nodes grow into the oxygen-stabilized alpha layer with relatively slow growth along the surface. The growth rate, along with the associated hydrogen uptake, is enhanced by partial and through-thickness cracking of the nodes. At 1000°C, the nodes grow rapidly along the E110 surface, interconnect, crack, delaminate and spall at relatively low test times. The hydrogen uptake is >100 wppm after a hold time of ≈300 s and >500 wppm after a hold time of ≈600 s at 1000°C. During the transition from initiation of breakaway oxidation to extensive delamination and spallation, the hydrogen content shows significant variation in the circumferential and axial directions: the concentration is high under regions of cracked "white" oxide and low under regions of intact "black" oxide.

6.2 As-received E110 Cladding

The "cladding" received by ANL differs from the "tubing" in that its outer surface has been etched and anodized. Based on very limited testing, this finishing process does not seem to reduce the susceptibility of E110 to nodular and breakaway oxidation.

6.3 Polished and Machined-and-Polished E110 Tubing

The roughness of the as-received tubing is ≈0.4 μm. Polishing to ≈0.1 μm roughness had a very dramatic effect in delaying breakaway oxidation at 1000-1100°C. For polished samples oxidized in steam at 1100°C, no significant nodular oxidation was observed up to 16% ECR (≈1000-s hold time). For polished samples oxidized in steam at 1000°C, lustrous black oxide was maintained up to ≈400 s and hydrogen uptake >100 wppm was delayed until > 900 s. These results are sample-length-dependent, as the discontinuity at the sample ends appears to be an initiation site for monoclinic oxide formation.

6.4 Pre-etched E110 Tubing

Compared to other alloys pre-etched and oxidized at 1000°C, E110 exhibits a much more negative response to pre-etching. This response – monoclinic oxide film formed over most of the sample surface – appears to depend on the etching time and the concentration of HF in the etching solution. Also, the degree of monoclinic oxide surface coverage is more extensive for the as-received than for the polished samples. On the other hand, polishing of the pre-etched surface prior to oxidation negated the effects of the etching.